A STUDY OF THE EFFECTS OF HEAT TREATMENT ON DELTA-FERRITE IN CAST AUSTENITIC STAINLESS STEEL

By

PAUL DOUGLAS RATKE

Bachelor of Science

in Mechanical Engineering

Oklahoma State University

Stillwater, Oklahoma

1987

Submitted to the Faculty of the
Graduate College of the
Oklahoma State University
in partial fulfillment of
the requirements for
the Degree of
MASTER OF SCIENCE
December, 1988

A STUDY OF THE EFFECTS OF HEAT
TREATMENT ON DELTA-FERRITE
IN CAST AUSTENITIC
STAINLESS STEEL

Thesis Approved:

Delcie R. Durham
Thesis Adviser

C E Price

J K Good

Norman N. Durham
Dean of the Graduate College

ACKNOWLEDGMENTS

I wish to express my sincere appreciation to Dr. Delcie Durham for her helpful advice and guidance and to Dr. C. E. Price for his help and friendly encouragement throughout my graduate program. I also extend many thanks to Dr. Keith Good for serving on my graduate committee along with Dr. Durham and Dr. Price.

To the American Foundry Group of Tulsa, Oklahoma, who helped in the preparation of the investment mold and shared their knowledge on investment casting with me, I extend my sincere thanks. Appreciation is also expressed for the partial funding of this project which was provided through the More Oklahoma Science and Technology project from the EPSCOR program of the National Science Foundation.

Finally, I wish to thank my parents for the support, both financial and otherwise, which they have given me during both my graduate and undergraduate work at Oklahoma State. Without their contributions my education would not have been possible.

TABLE OF CONTENTS

LIST OF TABLES

LIST OF FIGURES

CHAPTER I

INTRODUCTION

Cast austenitic stainless steel is used very widely in situations where corrosion resistant castings are needed. The microstructure of these steels is actually a duplex structure containing both austenite and delta-ferrite. The presence of the metastable delta-ferrite yields several beneficial results. For example, the addition of delta-ferrite increases yield strength and ultimate tensile strength and decreases the tendency of a casting to hot tear. Delta-ferrite can also help in a round about way with resistance to stress corrosion cracking. This is due to the ease by which carbide particles will form in delta-ferrite pools thus preventing them from forming at the austenite grain boundaries.

It has been shown in the literature that the benefits of delta-ferrite in weldments are dependent on the morphology of the delta-ferrite present. While a weld is in effect a small casting, the solidification conditions are very different from those of the standard casting processes.

This investigation is aimed at studying the

casting microstructure. The goal is to draw some conclusions as to the similarities of the weld and casting microstructures and to observe any differences and changes which may occur in the various morphologies of the delta-ferrite during a standard solid solution heat treatment. This type of alloy is normally solid solution annealed to dissolve corrosion initiating carbides at the austenite grain boundaries.

To carry out the above investigation, a set of castings was made from CF-3M of know composition using the investment shell technique. The castings were sectioned and their microstructure was examined to determine what morphologies were present. The amount of ferrite was determined by both the manual point count method and by estimation from the Schoeffer diagram (ASTM A800). Specimens were then put through various heat treatment cycles and the effects of those cycles on the amount and shape of the various ferrite morphologies was observed.

CHAPTER II

STAINLESS STEEL INVESTMENT CASTINGS

Introduction

Close tolerances, good surface finish, and minimal follow-up machining explain the existence and the survival of investment castings from the Bronze age to the Space age. Investment casting is a very old and commonly used process known through history as the 'lost-wax' process. The oldest known investment castings date back almost 6000 years to the Shang Dynasty of China (Krohn 1984). The favor and use of investment casting pretty much died out during the Dark Ages. It was not used very extensively for any thing other than art work until early in the twentieth century when an Iowa dentist, B. F. Philbrook, used it in his dental practice to make gold inlays and crowns. Later, during World War II, the need for a process to manufacture precision parts quickly and with a minimum of waste was needed, hence investment casting was used and has been used continually since (Krohn 1984).

Due to economic reasons, there has been a demand in recent years for complex shapes which can be produced in

a near net shape condition. This need has sparked continual growth in the now strong investment casting industry. At the same time there has been a demand for investment castings that have greater metallurgical strength and integrity along with a push for reduced weight (Helmer 1986).

Nature and Use of Investment Castings

Investment castings can be held to much more exacting tolerances than can sand castings. Normal linear tolerances for an investment casting are on the order of +-0.010 in.(0.0254cm) for up to 1 in.(2.54cm) and +-0.005 in.(0.0127cm) for each additional inch, while thin walls must have a minimum tolerance of +-0.020 in.(0.0508cm). However, investment castings are by nature no stronger or no more sound than are the more traditional sand castings (Broad 1967). Further, the size is normally far more limited for investment castings than for a sand casting. The manual manipulation necessary for shell preparation is normally the limiting factor for the size of investment castings. As the use of robotics increases in the foundry the maximum size will certainly increase leaving the strength of the shell itself as the main limiting factor (Krohn 1984).

Investment castings in general are used in almost every industry and can be cast of almost every metal or

alloy.

A survey reported by Helmer found that investment castings normally replace components that had previously been manufactured by way of significant amounts of machining or grinding. The advantage of this near net shape casting process is that sand castings, weldments and forgings are often replaced by investment castings (1986). Austenitic stainless steels, which are difficult to weld and to machine, provide an example of a material which is well suited to the investment casting process.

Refining, chemical, nuclear, plastics, and food industries are just a few of the industries which make broad use of investment cast stainless steels. Some examples of the types of applications are: mixer parts, pump casings and impellers, valve bodies, hydraulic and pneumatic components, nuclear power components, medical instruments, implants and prosthesis equipment, marine propellers, and food production equipment. (Helmer 1986, ASM 9:3)

Investment Casting Process

There are two different processes typically referred to as investment casting processes. The older of the two is the 'block method'. In this method the wax pattern is encased in a block of plaster or refractory. The other and more modern method

is the 'shell method' in which a refractory shell is built-up around the wax pattern in successive layers. The later version is now by far the more common and will therefore be described in more detail.

The process by which the investment shell is built-up is shown schematically in Figures 1 and 2. The large numbers in the figures indicate the order by which the steps are performed. It should be noted that steps three and four, dipping in the slurry and stuccoing with refractory, are repeated as many times as is necessary to build-up the desired shell thickness.

The slurry is usually made of very fine refractory, fused silica or zircon, suspended in a liquid which often contains water, ethyl silicate, defoamers, dryness indicators, and mild acids (Kalpakjian 1984). The refractory stucco is normally either fused silica or zircon sand of various grades. The inner layers of the shell are stuccoed with a fine grade of refractory while the outer layers, the backup layers, are stuccoed with a coarse grade of refractory.

After the shell is complete and the wax is removed as shown, the shell is fired to 'set' the refractory and remove any water which may be in the shell. Then the metal is poured into the shell and allowed to solidify. Often extra insulation, such as Kayowool, is added to the outside of the mold to impede solidification in the risers. Finally, after the metal is solidified and

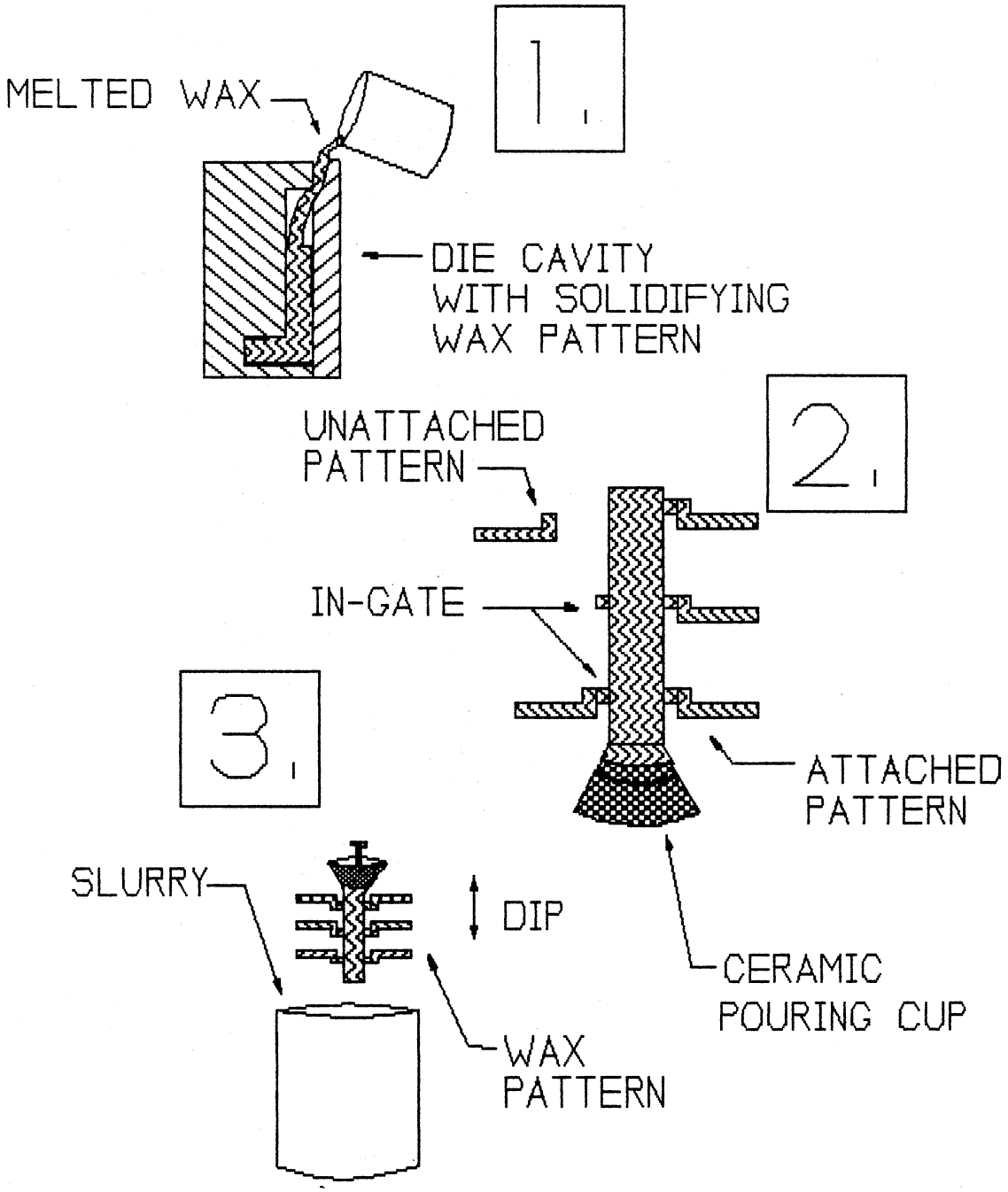

Figure 1. Schematic representation of steps 1 through 3 of the investment casting process.

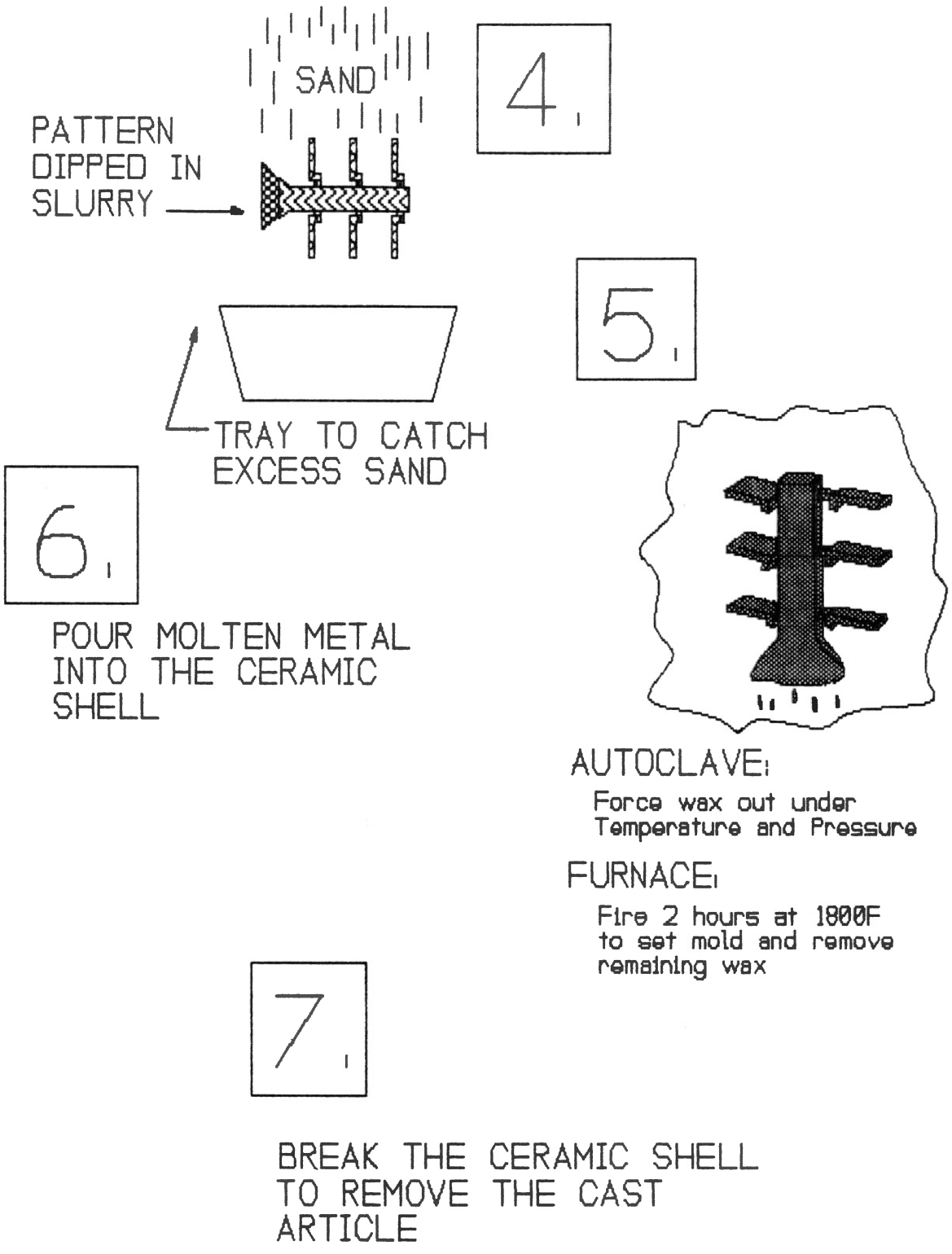

Figure 2. Schematic representation of steps 4 through 7 of the investment casting process

cooled down the ceramic mold is removed. Often this is quite a task in itself requiring shot blasting, caustic baths and great amounts of manual labor. The parts are then removed from the connecting gates and these areas are finished smooth by grinding. Normally, all that is left is to inspect the part and the process is finished. Final machining of some cast parts may be required, however this is kept to a minimum by proper casting design.

CHAPTER III

MICROSTRUCTURE OF CAST AUSTENITIC STAINLESS STEEL

Introduction

In 1910 it was discovered that when about 12% chromium is added to steel it will impart corrosion and oxidation resistance to the steel. It is from this discovery that the modern stainless steels, including CF-3M, have been developed. Definitions of stainless steels vary but for the most part it is agree that stainless steels must have a chromium content greater than 11 or 12 percent and must exhibit passivity (Weiser 1980, Budinski 1983).

There are many grades of cast stainless steel alloys available today. The microstructure of the various alloys play a considerable role in the corrosive and mechanical properties of these alloys. The rest of this chapter will identify CF-3M among the other stainless alloys, layout some general casting structures, and outline some of the theories which have been reported in the literature concerning the solidification of the cast austenitic stainless steels.

Characterization of CF-3M

The alloy, CF-3M, which is used in this study is the cast equivalent of the wrought alloy 316L. It is important to point out that it is the corrosion equivalent and not the same alloy with respect to composition or structure (Weiser 1980). Table 1 summarizes the composition and properties of these two alloys. The CF grade alloys are the most technologically important and highest tonnage alloys of any of the corrosion-resistant casting alloys in production (Weiser 1980, Budinski 1983). These alloys have good castability, weldability and are tough and strong down to -423°F(-253°C) (Weiser 1980). The 'C' in the designation refers to resistance to aqueous corrosion. The second letter indicates the amount of nickel, 'A' being the lowest and 'Z' being the highest. The numeral indicates the maximum amount of carbon and any additional letters indicate additional alloying elements. In the case of CF-3M, the 'M' indicates molybdenum (Weiser 1980) CF-3 and CF-3M are design for maximum corrosion resistance after field welding, with the molybdenum in CF-3M adding additional resistance to reducing environments.

While the wrought equivalents of the CF alloys are fully austenitic, the cast alloys actually posses a duplex structure of ferrite pools in an austenite matrix. These ferrite pools increase the corrosion

TABLE 1

COMPARISON OF CF-3M AND 316L

Composition		
Constituent(%)	CF-3M	316L
Cr	17.0 - 21.0	16.0 - 18.0
Ni	9.0 - 13.0	10.0 - 14.0
Mo	2.0 - 3.0	2.0 - 3.0
Si	1.5 max	1.0 max
Mn	1.5 max	2.0 max
P	0.040 max	0.045 max
S	0.040 max	0.030 max
C	0.030 max	0.030 max

Mechanical Properties		
	CF-3M	316L*
Tensile Strength ksi (MPa)	80 (552)	90 (620)
Yield Strength (0.2% offset) ksi (MPa)	38 (262)	45 (310)
Elongation in 2in. %	55	30

* Cold finished and Annealed bar.
Properties from (Weiser 1980) and (ASM 9:3)

resistance considerably by providing preferential nucleation sites for any complex chromium carbides which may form. These carbides, which precipitate in the temperature range between 800°F(425°C) and 1600°F(870°C), will also form at grain boundaries when ferrite pools are not available (Unterweiser 1982). CF-3 and CF-3M further improve the corrosion resistance by specifically limiting the carbon content to a 0.03 maximum in order to reduce the carbide precipitation at grain boundaries. They have a reduced susceptibility to selective, intergranular attack under normal conditions in the as-cast structure. However, under severe corrosive conditions, or if the casting has been weld repaired, it may be necessary to heat treat these grades to provide the optimum corrosion resistance (Unterweiser 1982).

General Cast Structures and Defects

Before a logical discussion of the solidification structures found in austenitic stainless steels can be initiated, a bit of general cast structure information must be laid out. The major points to understand about cast structures are dendritic solidification, and the formation and cause of defects such as shrinkage, and the various types of porosity, such as interdendritic and gas porosity.

The mechanical properties and the other properties

of a casting are greatly dependent on the structure. The structure in turn is dependent upon the process by which it solidified. Therefore, the mechanical properties are dependent upon the solidification process.

Two major categories of solidification processes exist. The first is freezing by skin formation and the second is dendritic solidification. Freezing by a skin formation is generally limited to pure metals or alloys solidifying under extreme conditions of thermal gradients; therefore, this discussion will center more around dendritic solidification which is the mode of solidification in CF-3M and many other alloys.

The formation of columnar dendrites is shown in Figure 3 following a changing pattern as the growth increases. The sequence begins at the mold and advances toward the interior in a nucleation wave which corresponds to the space between the isotherms equal to the solidus and liquidus temperatures. Initially, regular cells begin to grow perpendicular to the solid-liquid interface. Then, the growth deviates into preferred orientations which are determined by the direction of the heat flow. Next, the cross-section deviates from circular and serrations appear. Secondary arms are discernable and begin to increase in size. Finally, equiaxed dendrites start to form ahead of the columnar dendrites and complete the solidification

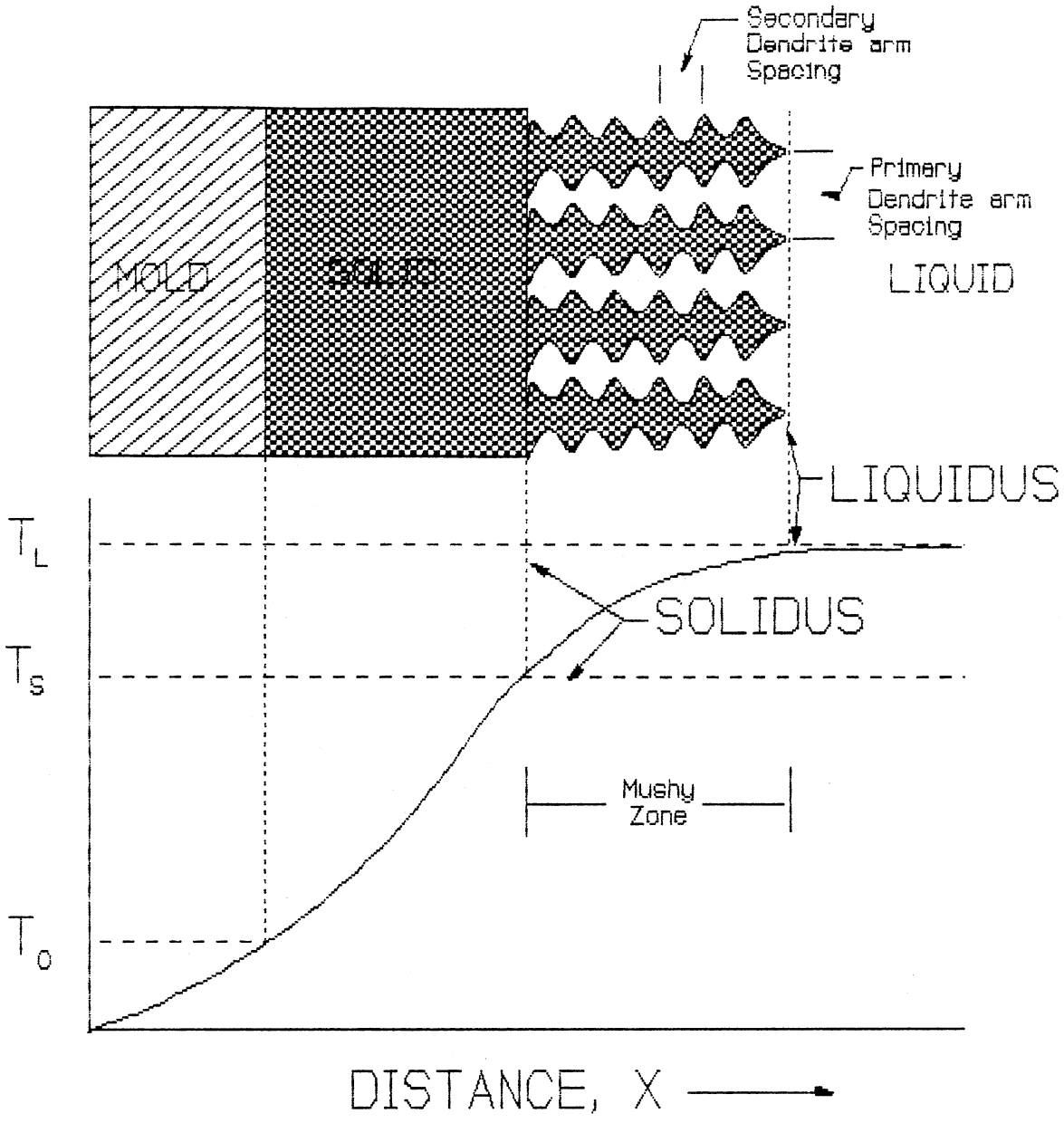

Figure 3. The Relationship Between Dendritic Growth and the Corresponding Temperature Profile

pattern. The final arrangement of the columnar and equiaxed structures is shown in Figure 4.

In an alloy, dendrites form as a three-dimensional structure. The initial dendrite structure has a composition low in solute. This causes the enrichment of the liquid surrounding the dendrite in the constituents which are not the first to solidify. As solidification continues the surface composition varies from the composition at the dendrite cores. This results in the segregation of constituents within the solidified dendrites, which is termed a cored dendrite. The degree to which diffusion tends to homogenize this segregation is highly dependent upon the cooling rate and composition gradients.

It can be further inferred that if the cooling is very extreme and the solidus and liquidus are very close together then the solidification pattern will approach that of the more simple skin formation pattern which results when a metal freezes at a point rather than over a range. This results in a much finer grain size and a more homogeneous structure. This distance is also affected by constitutional factors. In general, the band width is narrow when the thermal conductivity of the metal is relatively low, the mold has high chilling power, and the freezing temperature is high (Ruddle 1957).

So far, the formation of dendrites has been looked

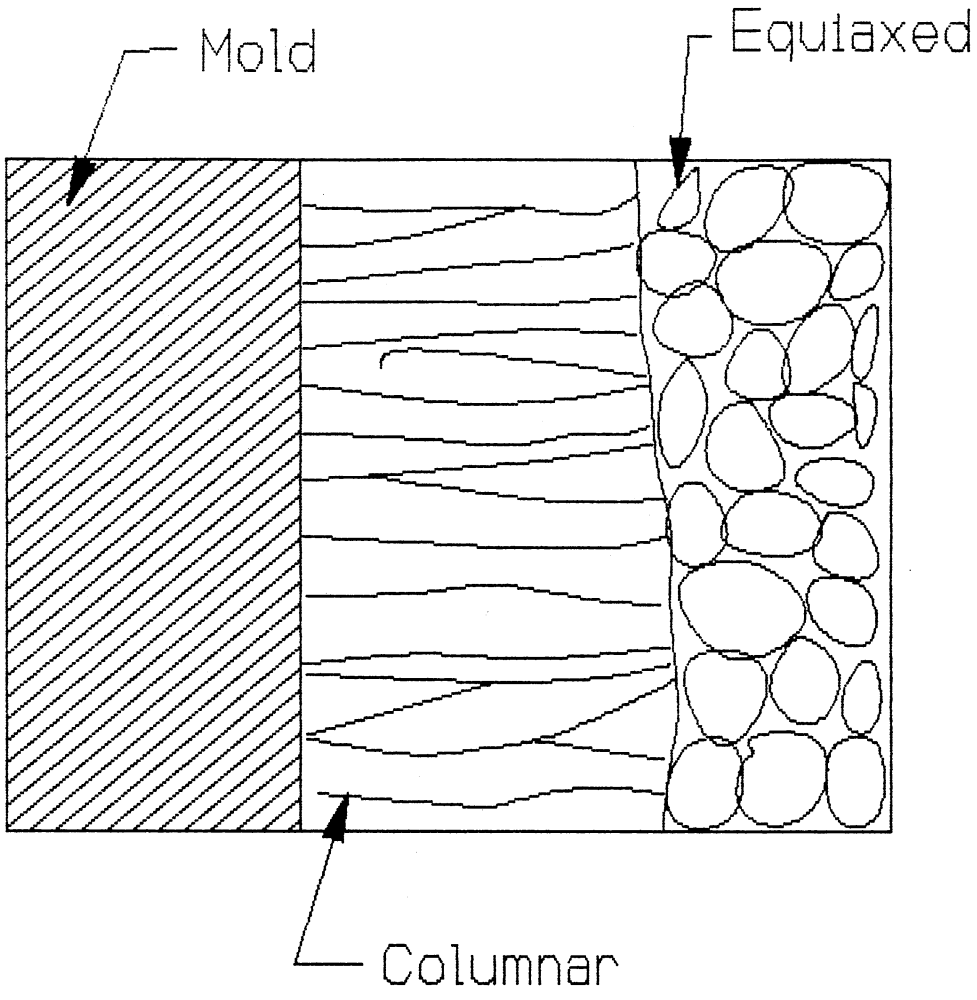

Figure 4. The Final Arrangement of Columnar and Equiaxed Structures.

at in general and the effects of constitutional and physical changes have been outlined. The actual difference of dendrite morphology can now be discussed. The actual shape of dendrites is, in fact, largely unchanged over a wide range of cooling rates. The only difference being that the structure simply becomes finer as the heat is extracted at greater rates (Flemings 1974). This indicates that some conclusions may be drawn about the solidification rate and cooling rates from the final as-cast structure. This is the case and the following considerations are used. Primary dendrite spacing depends on the gradient and the growth rate. Secondary dendrite arm spacing depends on the cooling rate and has been shown to be a good indicator for a wide variety of alloys (Flemings 1974). These spacing are shown schematically in Figure 3.

While the structures which result due to solidification patterns are important and have a great affect on the resulting mechanical and corrosion properties of a casting, defects which form in castings also play a very large role in determining the properties of the castings. Defects which may occur include, shrinkage, porosity, inclusions and hot tears. Major shrinkage problems can normally be prevented or held in desirable locations by feeding practices and directional solidification toward hot spots (Bralower 1988). Microshrinkage, however, is more difficult to

get around. It is shrinkage which is dispersed throughout large areas of the casting and is usually initiated in the interdendritic regions (Brawlower 1988). This type of shrinkage can cause very severe problems in a casting when a portion of the casting is machined away exposing a portion of the casting which contains microshrinkage to a corrosive environment. In this situation the shrinkage site will provide good locations for corrosion to get started. This type of shrinkage is also commonly known as shrinkage porosity and has been found to be affected by the shape and width of the solidification band (Ruddle 1957). Another common defect in large flat castings, while not so common in high alloy castings, is centerline porosity. Centerline porosity is closely related to insufficient interdendritic fluid flow. It has been shown that the pressure required to feed the shrinkage increases very rapidly as casting length increases. As a result, even increased casting pressure can do very little to alleviate this problem. Further it has been shown by Minakawa and others that it is possible to predict this type of shrinkage from the temperature gradient and the rate that the solidification front is moving through the casting (Minakawa 1985).

Inclusions are another form of defect. They are simply small pieces of foreign material which are trapped in the interdendritic regions of the cast metal.

The foreign material may be molding material which was entrained in the flow of molten metal, slag, or simply small pieces of 'trash' of unknown origin. Regardless of the origin of the inclusions, they reduce the quality of the casting since they reduce the strength of the cast material and may provide preferential locations for crack initiation and for the start of corrosion. They may cause the rejection of the casting altogether or may require subsequent removal by grinding followed by repair welding and heat treatment.

The final major casting defect to be considered is the hot tear, which is a tear in the casting which occurring while the casting shrinks during initial cooling. They are normally caused by a combination of low hot strength of the metal and excess rigidity of the molding media.

To reiterate, the microstructures and the presence and type of defects present can have a profound effect on the mechanical and corrosion properties of a casting. Therefore, it is necessary to understand and take in to consideration the aspects of the design and the process that can yield beneficial results in these areas.

Solidification Process of Austenitic Stainless Steels

Austenitic stainless steels, including CF-3M, follow the general solidification processes outlined in

the previous section. However, there are several theories as to how the structures get from the dendritic solidification structure to the duplex structure of delta ferrite pools in an austenite matrix which is present in the as-cast structure at room temperature. While these theories are not exactly the same, they do have similarities; therefore, they will now be presented and brought together where possible.

The rate at which the solidification front moves through the casting affects the amount of ferrite formed; therefore, this would indicate that prediction of the amount of ferrite present in the cast structure merely from the composition is inherently inaccurate (Lippold 1979). However, the process or rather the mechanism by which the ferrite forms is not nearly as dependent on the rate at which heat is transferred from the casting. Therefore, the solidification theories are useful over a wide range of circumstances.

Originally it was assumed that the duplex structures containing a small volume percent ferrite had solidified initially as austenite with ferrite distributed along cellular dendritic boundaries. However, it was also recognized early on that when the amounts of ferritizers or the amounts of austenizers are altered the primary solidification phase must sometimes be ferrite (Lippold 1979). This is in fact the case with many of the duplex alloys including CF-3M. Figure

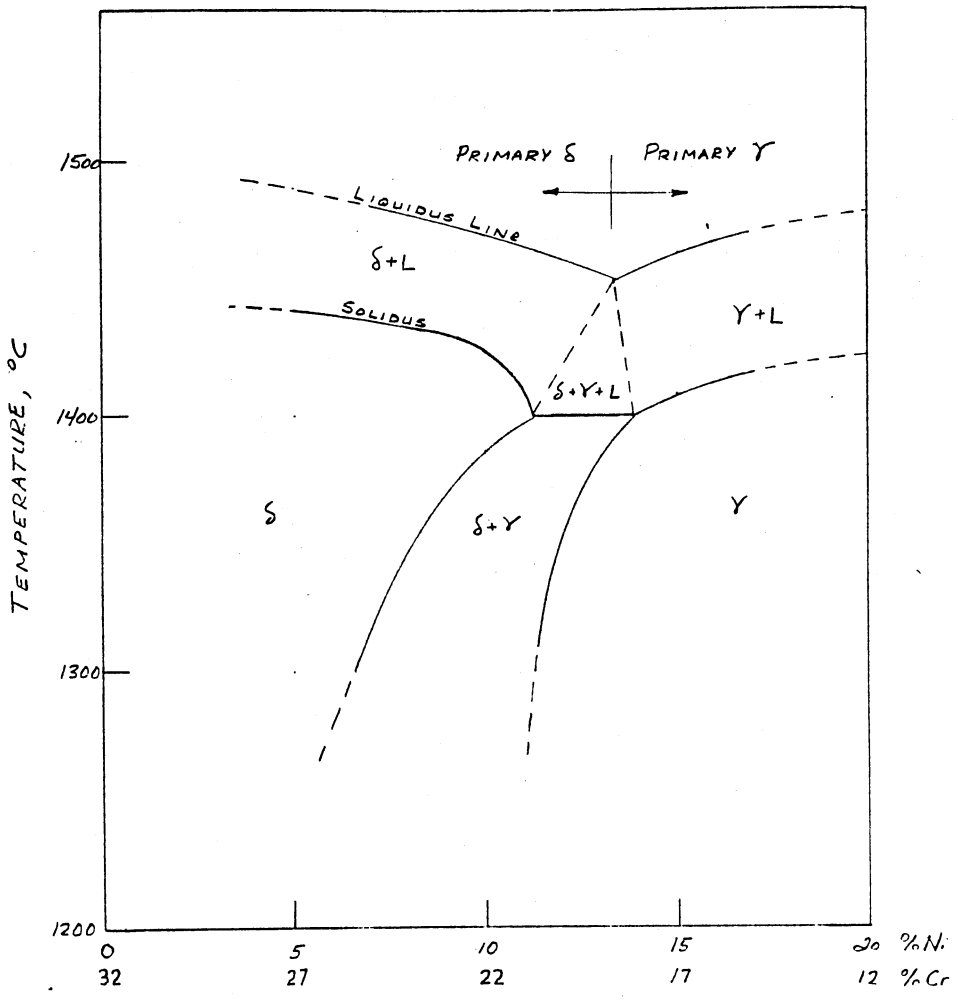

Figure 5. Pseudo-Binary phase diagram for 68% Fe. (Leone 1982)

5 is a pseudo-binary phase diagram developed from the tertiary iron-chromium-nickel system. This diagram was set up by Leone to have a fixed 68 percent iron, thus allowing the chromium and nickel to vary as a binary system would (Leone 1982). It can be seen from this diagram that alloys on the chromium rich side form a primary solid phase of delta ferrite. Alloys on the nickel rich side form a primary solid phase of austenite. Since CF-3M belongs to the group of alloys whose primary solidification structure is delta ferrite, At temperatures just below the solidus, primary delta ferrite forms. This ferrite will be at the cores of the forming dendrites and will have the approximate composition of ferritic stainless steels. This initial ferrite is usually approximately 26 percent chromium and 4 percent nickel. This means the cores of the dendrites are very enriched in ferritizers and depleted in austenizers (Lippold 1979).

Electron probe microanalysis has supported this part of the theory and has successfully shown that the cores of the original ferritic dendrites are very rich in chromium. This high chromium content gradually decreased further away from the cores of the dendrites while at the same time the amount of nickel increased (Leone 1982, Lippold 1979). Now the question arises as to how the ferrite which initially solidifies can become at room temperature a matrix of austenite with discrete

pools of ferrite dispersed throughout. This is an area of some debate; however, some of the more recent papers seem to have laid out some fairly logical conclusions. Lippold and Savage say that the microsegregation that is present at room temperature is produced during the liquid to solid transformation with no further redistribution of elements below the solidus (Lippold 1979). This theory has a problem in that it does not fully explain the resulting structures. In other words, this theory adequately explains those regions of the structure where there is strong dendritic growth however it does not account for those regions where there are clusters of lacy ferrite pools surrounded by solid areas of austenite, this theory falls short. Leone holds a contrary view, proposing that the ferrite to austenite transformation is diffusion controlled and continues even below the solidus. He proposes that the distribution of the alloys occurs partly in the liquid and partly in the solid due to decomposition of delta ferrite to austenite. The primary solidification occurs as either liquid to ferrite or liquid to ferrite plus austenite, then a ferrite to austenite transformation begins to take place. This transformations begins even before solidification is complete and continues well below the solidus (Leone 1982). He goes on to explain the lacy structure which occurs by concluding that the austenite which forms in the liquid envelopes the

solidified ferrite then begins to grow into the ferrite pools even as the majority of the ferrite itself is transforming to austenite.

Most of the research done on ferrite formations in austenitic stainless steels has been conducted in the studies of welding. A weld bead is a small casting and often there are similarities in microstructure, dependent upon materials and process similarities (Leone 1982). Therefore, an extension into ferrite formation in cast structures may well show similarities to welds under the appropriate conditions.

Microstructure and Its Development

This section will outline the morphologies which are expected in the CF-3M microstructure. It will also present the documented effects of heat treatments on weld metals in order to establish the possible effects of heat treatment on the cast microstructures.

Figure 6 is a micrograph which was published in the ASM Handbook of Metals. It is of a sample of CF-3 which of course is for most purposes and identical structure to that expected in CF-3M. In this micrograph the discrete pools of delta ferrite are clearly visible in the austenite matrix (ASM 9:9).

Takalo et al. reported only two morphologies, the first being a soft form and the second being a needle-like form (Takalo 1976). While on the other hand,

Figure 6. Cf-3 alloy, as-cast showing dispersed islands of ferrite in an austenite matrix. Copied with permission from the ASM Metals Handbook ninth edition, volume 9.

David, who seems to have studied the matter in more detail, has report four distinct and separate morphologies which are developed due to thermal and compositional variations (David 1981). Examples of the four reported morphologies can be seen in the four parts of Figure 7. With some interpretation of the descriptions provided by these investigators, it is clear that the four morphologies reported by David can easily fit into the two, more general groups, reported by Takalo and the others. This can be done as follows, the morphologies of Figure 7 parts A, B, and D could easily fall into Takalo's soft form group while the morphology in part C is most definitely the needle-like structure reported by Takalo.

Since the apparent differences have been settled, a more in depth discussion of the various morphologies is now warranted. To reiterate, David reports four distinct morphologies. He shows that they are not simply different views of the same three dimensional structure. He then names the various structures and gives arguments to the possible sources of these structures. The structures which he reported on were all found in the weld metal of 308 stainless steel. The first structure, shown in Figure 7a, is termed the 'Vermicular' morphology. The second, Figure 7b, is the 'Lacy' morphology. The third, Figure 7c, is the 'Acicular' morphology and finally the fourth, Figure

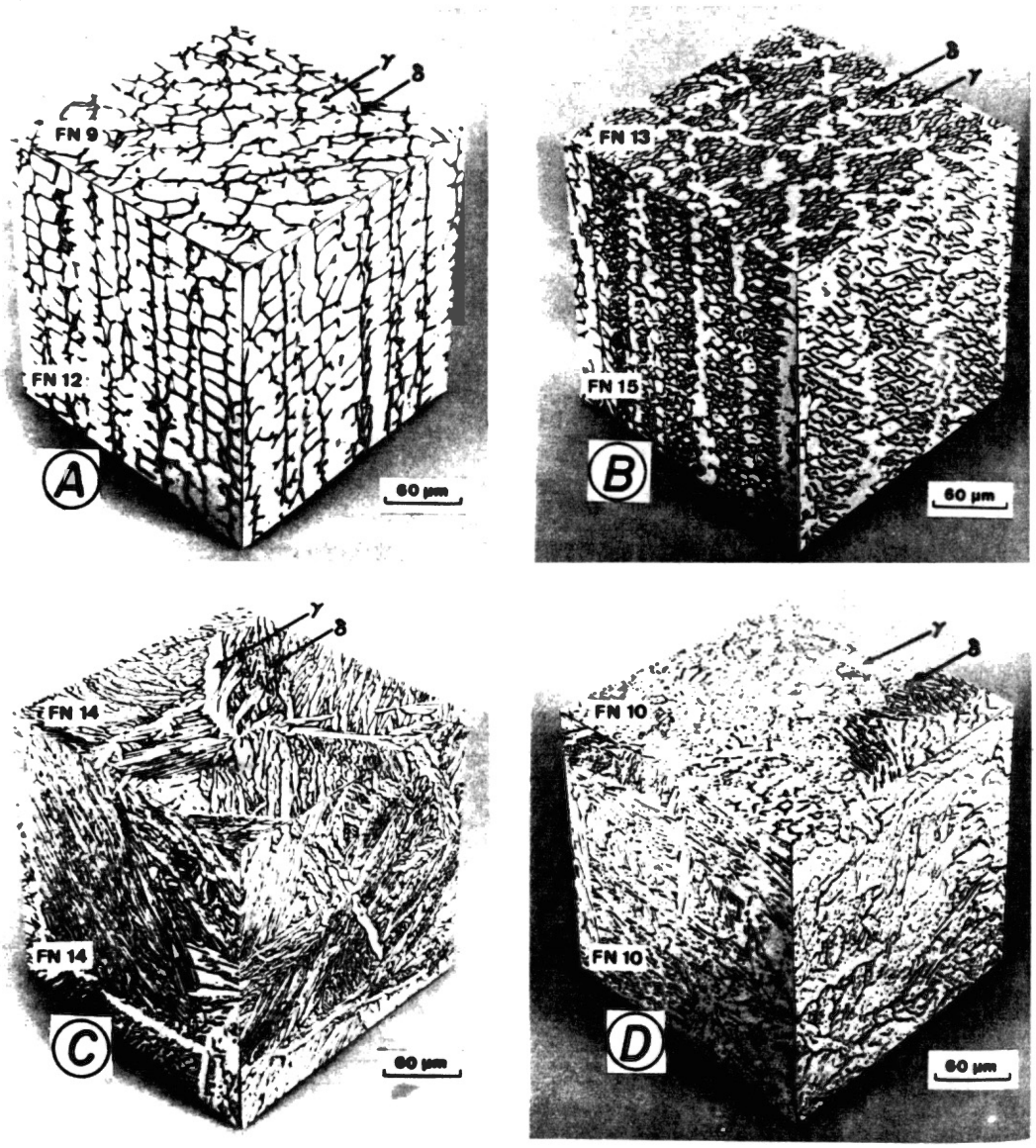

Figure 7. Three-Dimensional composite micrographs of the four distinct morphologies present in the weld metal of 308 stainless steel. Copied with permission from David 1981.

7d, David has called the 'Globular' morphology. These names appear to be adequately descriptive of the structures and will be used in this paper to identify the various structures as needed.

The vermicular morphology is characterized by an aligned skeletal network or curved soft form depending on orientation. The general alignment of the network is along the heat flow direction. The ferrite present is the remnants of the primary and secondary dendrite arms and is the result of an incomplete transformation of delta ferrite to austenite during solidification and cooling (David 1981, Suutala 1980). The cores are left and the structures are formed because during the cooling the high surface area to volume ratio of ferrite causes it to try to spherodize. The spherodized regions eventually shrink back toward the cores of the primary and secondary ferrite arms. This process can account for the soft, rounded vermicular pattern. The spacing between the branch-like lines can be measured and is equivalent to the spacing of the original delta ferrite dendrite arm spacing (Leone 1982).

The lacy morphology is characterized by an interlaced ferrite network oriented along the growth direction. It is likely formed by the transformation of primary delta ferrite to austenite and ferrite. This part of the transformation is described in the previous section and is further discussed by Leone. Leone

reasons that this structure is taken to represent the point at which the austenite has enveloped the solidifying ferrite and grew in both directions, both into the liquid and into the ferrite which already formed at this point (Leone 1982). The arrows on Figure 7 indicate the position of this austenite and ferrite.

The acicular morphology is characterized by a random arrangement of needle-like ferrite distributed in an austenite matrix. It was found only in the last passes of the weld metal and is attributed to local variations in the composition (David 1981). This morphology is therefore not expected in an as-cast structure. Several investigators have identified a similar structure and have attributed it to a Widmanstatten type process. They found it to occur in areas which were quenched from liquid down to room temperature (Fredriksson 1972, Leone 1982).

The final morphology discussed by David is the globular morphology. It is characterized by ferrite in globules which are randomly distributed in a matrix of austenite. The structure has no directionality and is found in the weld passes which are severely heated by subsequent passes. It was therefore reasoned that the origin of this structure must be due to the thermal instability of the other structures (David 1981). This again indicates that this structure will also probably not be found in the as-cast structure. However, there

is a great likelihood that this will be a prevalent structure found after heat treatment.

An important point made by David is that contrary to past suggestions the increasing or decreasing the cooling rate can not alter the amount of delta ferrite which is present in the austenite (David 1981). This however, must obviously be referring to some reasonable range of cooling rates. He goes on to explain that for higher solidification rates the finer spacing of the dendritic substructure allows for the same amount of ferrite volume but with considerably more surface area. This would indicate that differences could be seen on subsequent heat treatments. However, these difference will likely be small and they should probably not be expected in the same casting since there will be compositional variations due to segregation of elements during solidification.

Heat Treatment of Cast Austenitic Stainless Steels

Since no mechanical strengthening is possible through heat treatments, the heat treatment of the austenitic grades of cast stainless steels is done solely for the purpose of increasing their corrosion resistance. They achieve their maximum resistance to intergranular corrosion by the high temperature heating and quenching procedure known as solution annealing.

The purpose of this process is to insure complete solution of the chromium carbides in the austenite matrix and to retain these carbides in solution (Boyer 1982, Weiser 1980). A further advantages to the corrosion resistance is provided by the duplex structures of the steels such as CF-3M. This advantage is the delta ferrite pools which act as preferential precipitation sites for any carbides which do precipitate.

Standard heat treatments for CF-3M have been set out by ASTM and the American Society of Metals. ASTM specification A743 indicates that a CF-3M casting should be heated to a minimum temperature of 1900°F(1040°C), held for a sufficient time to heat the casting to temperature and then cooled rapidly so as to develop acceptable corrosion resistance (ASTM,A743). The practice recommended by ASM in the Metals Handbook is the same procedure as given by ASTM except the upper temperature of 2050°F(1120°C) is quoted and the quenching media is specified as water, oil or air (ASM 9:3).

During heat treatment there are several points that must be considered. If the surface is to be preserved, precautions should be taken to prevent alloy depletion and scaling on the surface. This may mean that an inert environment will be called for (Garrow 1966). Precautions to minimize distortion, the heat treating

temperature and time, and control of the quenching media must also be considered to make any reliable heat treatments. It has been reported in industry that some large heat treating furnaces have temperature variations in the chamber that range as high as 25°F(14°C) from the set point (Garrow 1966). A concern that is often seen in industry is that some carbides deep below the surface may be left due to too short of heat treating cycles. These carbides will certainly cause heat treating problems if these area are exposed to the environment by a machining operation.

While the main purpose of the heat treatment cycle is to eliminate carbide particles which may allow initiation of intergranular corrosion, the metastable pools of ferrite are also affected. David reports that all four of the morphologies he classified showed extensive degradation of the ferrite structure after just 10 minutes at 1922°F(1050°C). He reported a simultaneous dissolution and change of shape in which the other morphologies tend to assume the globular morphology. He made the conclusion that if given sufficient time, a complete dissolution of the ferrite would occur in the 308 weld metal he examined (David 1981).

Since the ferrite dendrites are very fine and are quite strongly segregated in chemical composition and in a nonequilibrium state, it follows that any thermal

treatments which allow some reasonable diffusion could appreciably modify the size, shape and quantity of delta ferrite (DeLong 1974). While several authors have developed models which attempt to explain the phenomena of ferrite dissolution, few have been successful. The process is very complex since there are several elements diffusing in several directions through two different types of lattice structures which have resistance to diffusion that differs by two orders of magnitude (Moharil 1974). In one study it was found by electron probe analysis that the level of chromium increases in the ferrite and the nickel decreases during heat treatment. It was reasoned that these changes were related to the specific sequence of transformations that the ferrite undergoes before it disappears (Raghunathan 1979).

While a complete model or analysis of the actual dissolution process must be complex by its very nature, the process was expressed by Raghunathan in a simple form by the following pseudo-rate equation:

$$f/f_o = C - K_D \log t \qquad (1)$$

where: f - percent ferrite remaining
f_o- percent ferrite initially
t - time of heat treatment
K_D- temperature dependent rate constant
C - intercept on the ordinate of the f/f_o vs log t plot

Raghunathan went on to express the K_D as a function of

temperature with the following equation:

$$K_D = K_{D_o} \exp(-Q/RT) \qquad (2)$$

where: K_{D_o} - pre-exponential factor
Q - activation energy for the process
R - ideal gas constant
T - absolute temperature

It should be noted that this equation has a form similar to that of the Arrehnius equation. However, in this equation the K_D is not a pure diffusion coefficient.

The Effects of Delta Ferrite on Properties

Delta ferrite is beneficial in three major areas: providing strength, improving weldability, and maximizing the resistance to corrosion in specific environments. The effects of delta ferrite will be discussed in a little more detail then the methods of measuring the delta ferrite will be outlined.

Strength along with several other mechanical properties are improved; but, the mechanical properties of the CF alloys are usually secondary considerations to corrosion. Due to the flexibility allowed by the standard compositions which were designed with corrosion in mind, a wide range of mechanical properties are attainable. Strengthening of the CF alloys is limited to that which can be gained by incorporating ferrite in the austenite matrix; because, they can not be strengthened by thermal treatment, hot or cold working

or carbide precipitation which would be detrimental to the corrosion resistance in aqueous environments. Incorporation of delta ferrite improves the yield strength and ultimate tensile strength substantially without any loss of ductility or impact toughness at temperatures below 800°F(425°C) (Weiser 1980). According to Budinski this improvement of the yield strength may be as much as 100 percent (Budinski 1983).

The beneficial effects of delta ferrite in welds were first recognized in 1947 by Schaeffler who published a diagram which could be used to predict dilution effects in weld metals and choose welding electrodes (Campbell 1975). The main benefit that ferrite produces in austenitic weld metal is to lower the susceptibility of the metal to hot cracking and microfissuring.

Hot tearing may be directly prevented by delta-ferrite, since, it has been reported that when a minimum of 4% delta-ferrite exists in the structure the problem of micro-fissuring in welds can be reduced or eliminated. This suggest that hot tears in castings could possibly be reduced by the presence of delta-ferrite.

The only concern in welds with delta ferrite content is that if the percent delta ferrite gets too high it may begin to transform to brittle phase which can reduce corrosion resistance and lower mechanical

properties.

The CF grade alloys were designed and are usually called out for applications where corrosion resistance is the main concern. Therefore, it makes sense to now discuss the effects of delta ferrite on the corrosion properties of these alloys. The Duplex structure improves the resistance to stress corrosion cracking and to intergranular corrosion. The ferrite pools block the advance of cracks in both stress corrosion cracking and with cracks that form due to intergranular corrosion. The ferrite pools also act as preferential sites for carbide precipitation so that the carbides precipitate there rather than at the austenite grain boundaries (Campbell 1975). In fact according to David there is a critical amount of austenite-ferrite boundary area above which the alloy is immune to sensitization (David 1981).

According to the ASTM specification A800, there are three major types of measurement of delta ferrite. The first is by chemical composition, the second is magnetic response measurements and the third is the manual point count method (ASTM A800). The ferrite number is accepted index to quantify the ferrite content. It is closely related to the actual ferrite content and corresponds fairly well with the volume percent of the ferrite especially at low levels (Wieser 1980). The first method stated by ASTM is an estimation from the Schoeffer diagram based on the composition of

the steel. A Schoeffer diagram can be seen in Figure 8. The necessary fraction of chromium equivalent over nickel equivalent can be calculated from the following relations (ASTM A800)

$$Cr_{eq} = Cr\% + 1.5Si\% + 1.4Mo\% + Cb\% - 4.99 \quad (3)$$

$$Ni_{eq} = Ni\% + 30C\% + 0.5Mn\% + 26(N-0.02)\% + 2.77 \quad (4)$$

The main problem with this method is that the degree by which the constituents can be determined is somewhat limited in accuracy. However, the consideration must be made when using this method that it does not take into account any thermal history which can have a vast effect on the amount of delta ferrite present. The second method of measuring the ferrite content is by magnetic response. This method has the problem of device calibration and errors which may occur due to other magnetic phases which may possibly be present in an alloy. The magnetic response method is also somewhat dependent on the section size. The last method suggested by ASTM is the manual point count method. This method was used in this study and is described in some detail in the Appendix. ASTM specification A800 requires that the ferrite range after final heat treatment be called out in ordering. This may be difficult in that they give no feel of how much the ferrite will dissipate during heat treatment.

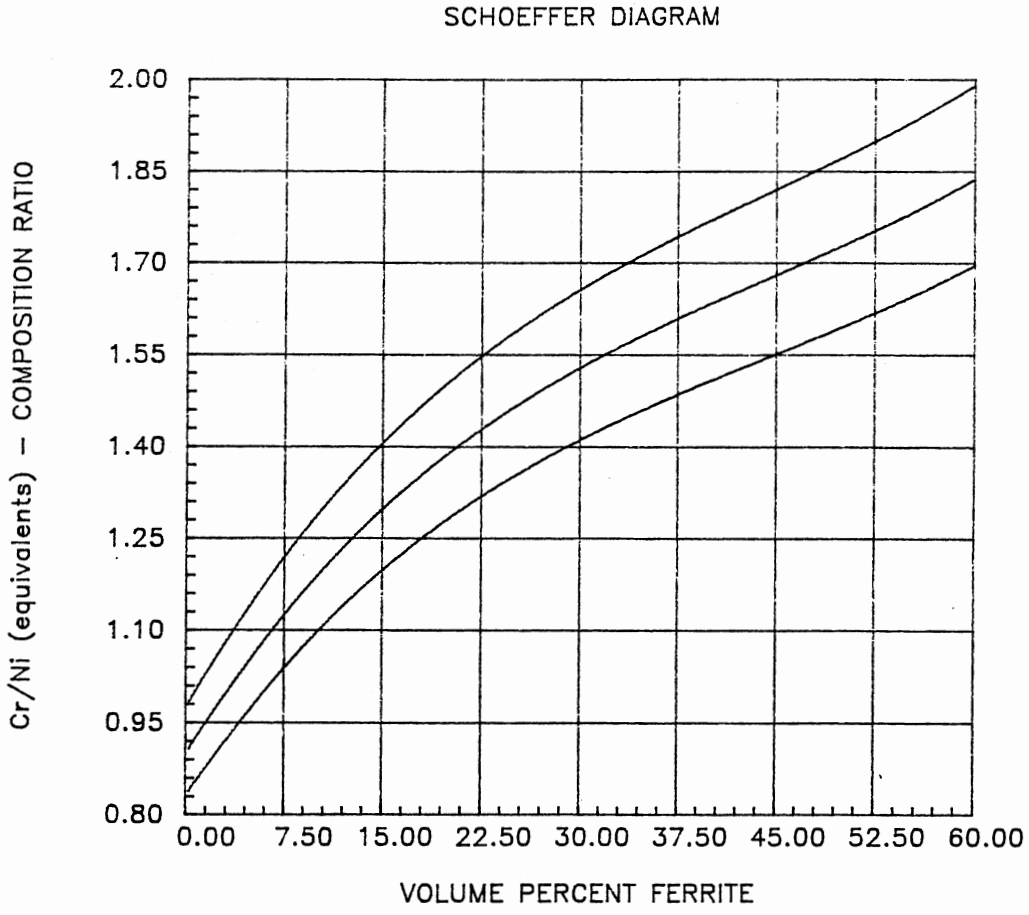

Figure 8. Schoeffer Diagram. (ASTM A800)

CHAPTER IV

EXPERIMENTAL PROCEDURES

Introduction

First, a casting design was derived which would allow for easy sectioning and evaluation. Next, wax patterns were designed and formed so that investment molds could be made in which to cast the test specimens. After the molds were prepared, the specimens were cast. Following cleanup and removal from the down sprue each of the specimens were sectioned and preliminary evaluations were made to determine what further sectioning could be done. The final sectioning was done to provide the number of specimens necessary for the heat treatment tests. Finally, the heat treatments were done and the specimens were prepared and evaluated.

This chapter is a discussion of each of the experimental steps. Details of the process are laid out and observations dealing with the processes themselves are presented.

Design of Casting Specimens

To perform any kind of responsible tests to determine the effects of various heat treatments on the

microstructure, it is necessary to produce castings in which the as-cast microstructures are very similar. To do this, a flat plate casting was designed. The plate has a riser at the end where the metal is gated in.

The diagram in Figure 9 shows the dimensions of the final cast specimen. Gating is done into the bottom of the riser, which actually is on the bottom of the casting. This is to provide some degree of bottom filling for the actual plate. The riser should cause a hot spot at the end of the casting and provide for a relatively sound casting elsewhere.

Since the casting specimens are small, approximately 3/4 lb.(0.34 kg), it is possible to place several of them on a tree so they may be cast simultaneously. This will provide the advantage that all of the specimens will be cast from the same melt. However, several disadvantages also arise. First, care must be taken to insure that the castings are far enough apart on the tree so that they do not interfere with the heat transfer of adjacent castings; and second, the effects of pressure head on the resulting as-cast microstructure must be considered.

Pattern and Mold Preparation

As discussed in the previous section, the wax patterns are to be connected in a tree fashion for

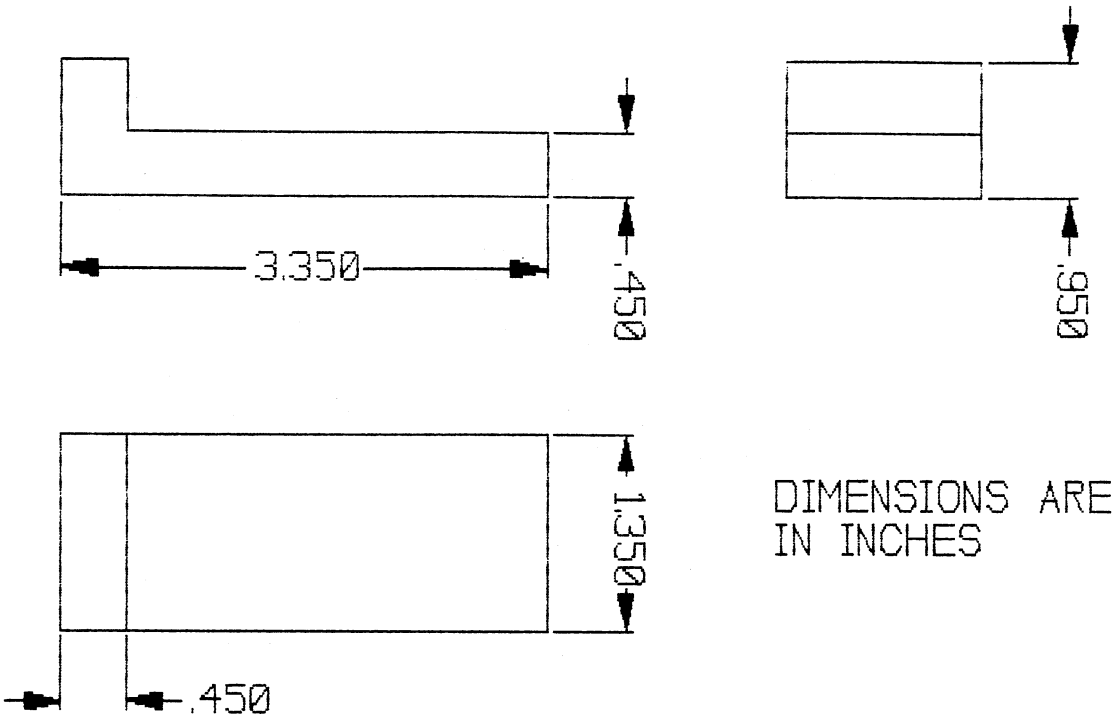

Figure 9. As-Cast Dimensions of Cast Specimen.

improved castability. Of course, before this can be done, the patterns themselves must be designed and formed. After this is done and the trees are assembled, the investment mold can be built-up around the pattern and processed into a mold capable of holding the molten steel.

The wax patterns were designed in the same general shape as the desired final casting specimens, with, of course, allowances for shrinkage. Then, the problem of forming the wax into the designed shape arose. The wax used was an unfilled foundry pattern wax with a melting point measured to be somewhere around 185°F(85°C); however, good fluidity is not achieved until temperature around 225°F(107°C). After some trial and error experimentation, it was determined that the best method of forming the wax is to cast it into a mold which has all of its surfaces made of the same material. A mold was made of a castable two-part urethane. This pattern mold along with one of the patterns is shown in Figure 10. In an industrial foundry the production pattern molds are usually made of aluminum and are filled with pattern wax that is under pressure. In this case, since only a few patterns were to be made, the mold was filled using only gravity feed. After inspection of the first few patterns, it was determined that this method would produce suitable results.

The next step in the process of producing the molds

Figure 10. Wax pattern and urethane pattern mold.

is to connect the patterns on to a down sprue to form a tree. The down sprue will have a ceramic pouring cup connected at the top and some means by which to hold the pattern tree during the investment process. In this case, six of the patterns were connected to a down sprue measuring 8 in.(20.32 cm) in height and 1.5 in.(3.81 cm) square. The patterns were connected to the sprue in such a manner as to reduce the heat transfer between the patterns as much as possible.

After the patterns are assembled into a pattern tree and the pouring cup and hanger are attached to the top of the sprue, the investment process can be started. The investment materials, used to produce the shell, were obtained from Ransom & Randolph; therefore, several of the components will be referred to by their trade names. This is necessary since they are complex solutions which cannot be easily described otherwise.

The first step in the investment process is to clean the wax pattern thoroughly. This is necessary so that the slurry will be able to wet the pattern and will not simply flow back off of it. A cleaning solvent sold by Ransom & Randolph as Genesolv was used to clean the patterns. This nonflammable solvent, which is an azeotropic combination of trichlorotrifluoroethane with acetone, ethanol, isohexane and nitromethane, cleans the patterns easily and allows the slurry to completely wet the pattern.

After the pattern tree has been cleaned using Genesolv, they are ready to go through the investment process. The first step in this process is to wet the pattern with a solution from Ransom & Randolph sold as Primcote. Primcote is actually a solution of suspended collodial silica which contains several other ingredients, such as defoamers, wetting agents and a drying indicator which changes color from green to orange as the solution dries. Primcote is also used as the base for the refractory slurries used in the next steps of the process.

After the pattern tree has been wetted in Primcote, it is ready to be dipped in the slurry. In general, the rest of the investment process follows the simple routine of: wet, dip in slurry, stucco with refractory, allow to dry. The slurries used contain Primcoat, and equal parts of -200 mesh zircon flour and -200 mesh milled silica. The refractories are either zircon sand, fine silica sand, or coarse silica sand depending on the coat being applied. A full listing of the various coats that were applied to the pattern is given in Table 2.

After the necessary number of layers of investment materials have been applied to the pattern, the shell is allowed to dry. Once dry, the wax pattern can be removed from the ceramic shell. This can be done by one of two methods. The first method is to flash fire the shell for enough time to allow the outside of the wax

TABLE 2

STEPS IN THE INVESTMENT PROCESS

1.	Pattern cleaned with Genesolv.
2.	- Wet with Primcoat. - Dipped in primary slurry. - Stuccoed with zircon sand.
3.	Repeat step 2.
4.	- Wet with Primcoat. - Dipped in backup slurry. - Stuccoed with -50, +100 mesh fused silica.
5.	Repeat step 4.
6.	Repeat step 5.
7.	- Dipped in backup slurry. - Stuccoed with -30, +50 mesh fused silica.
8.	Repeat step 7.
9.	Repeat step 8.
10.	Repeat step 9.

pattern to melt. Then the pattern can be melted out at low temperature. If the flash firing is skipped the ceramic shell will rupture due to the pressure generated by the expansion of the pattern upon melting at low temperature. The second method is to melt the wax out in an autoclave. The autoclave can remove the wax at a much lower temperature than is necessary for flash firing. This is due to the great speed at which energy can be added from the steam and also due to the pressure which can be applied which will help balance any internal pressure developed by the melting wax. The autoclave method was chosen. During the autoclave process there were some slight problems with cracking of the mold which resulted in two of the patterns breaking off of the tree. The holes which were left in the down sprue were patched with furnace cement and the shell was given a final coat of slurry to insure that any hairline cracks were filled.

During the autoclave cycle, most of the pattern wax was removed from the ceramic shell. To remove the remaining wax the shell was fired at 1800°F for two hours. In addition to removing the remaining wax, this step in the process also 'sets' the ceramic. Thus, the resulting shell is hard and strong and is porous enough to allow gases to escape through it. The ceramic shell investment process is now complete and the mold is ready to hold the molten steel. Figure 11 is a photograph of

Figure 11. Completed mold ready to be filled with molten metal.

a completed investment mold suitable to cast five specimens.

Casting of Specimens

The casting process is a very straight forward step in the process. In general, the mold is supported over a refractory bed in case of mold failure; then, the molten metal is poured into the mold. After the metal has solidified and cooled to room temperature, the casting is removed by breaking the investment mold. Finally, the specimens can be cut from the down sprue.

The variables which can be controlled at the casting stage of the process are the mold temperature, the casting temperature, and the amount of external insulation placed around the mold. External insulation is often used in the foundry to help isolate hot spots in risers and sprues thus allowing the usable portion of the casting to be more sound. In this case, no external insulation was used. The metal was poured at 2714°F(1490°C). The mold was at room temperature, approximately 75°F(24°C), this was done to chill the metal as much as possible to provide as fine a structure as is possible in an investment casting.

The cooling metal heated the mold to the point of glowing red in some spots. The cooling was allowed to occur naturally, it took about hour and twenty minutes from pouring for the temperature to be below

150°F(66°C). The casting was then removed from the mold by breaking the mold. As expected, the surface finish of the casting was not as good as is normal for investment castings. Had a good surface been desired rather than a chilled surface, the mold would have been preheated to about 1800°F(982°C). This would provide the exceptional surface finish normally associated with investment castings.

Specimen Preparation

After the specimens were removed from the down sprue, they were sectioned for preliminary microstructural evaluation. From this, the similarities of their structure and the extent of further sectioning could be determined. Final sectioning was done followed by the various heat treatment cycles and specimen preparation.

The four as cast specimens were sectioned along their vertical centerline, see Figure 12. After polishing and etching the sectioned surface, it was determined that the four specimens were very similar. Further, each of the specimens had a considerable length of almost identical structure. To compare the specimens, two general areas were considered. First, the percent volume of ferrite was estimated using the manual point count method, see the Appendix. Secondly, the general shape, size and distribution of the

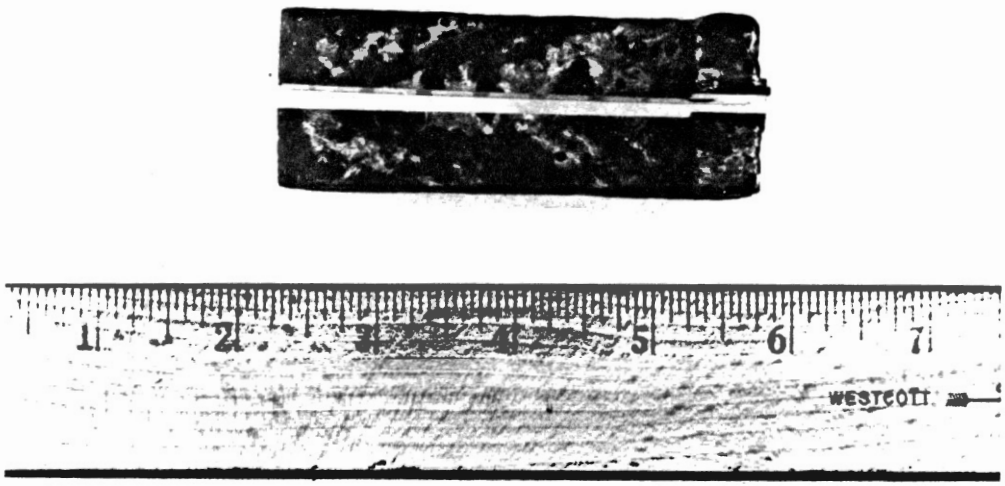

Figure 12. Cast Specimen Sectioned for Preliminary Evaluation.

structure was considered. The average volume percent ferrite of the four specimens fell within the same 95% confidence interval and there appeared to be no difference in the size, shape and distribution of the ferrite in the austenite matrix. These observations indicated that the four specimens, could be used interchangeably in the heat treatment tests. The other thing to be determined from the preliminary evaluations was to how the individual halves of the specimens could be sectioned. The point here is that the sections must be large enough so that a full representation of the structures found in the castings will be present in each section. While at the same time, the sections need to be as small as possible so that the maximum number of sections may be cut from each specimen. As was already stated above, the specimens had a long section in which there was no distinguishable variations in the structure. After examination of the microstructure, it was determined that if the riser portion of the casting was discarded, the specimen halves could be sectioned into a maximum of six sections each with each section still exhibiting a characteristic microstructure and a large enough surface on which to perform a reliable manual point count.

Four of the eight specimen halves were sectioned. With the other four reserved for other research. A fully sectioned specimen is show in Figure 13.

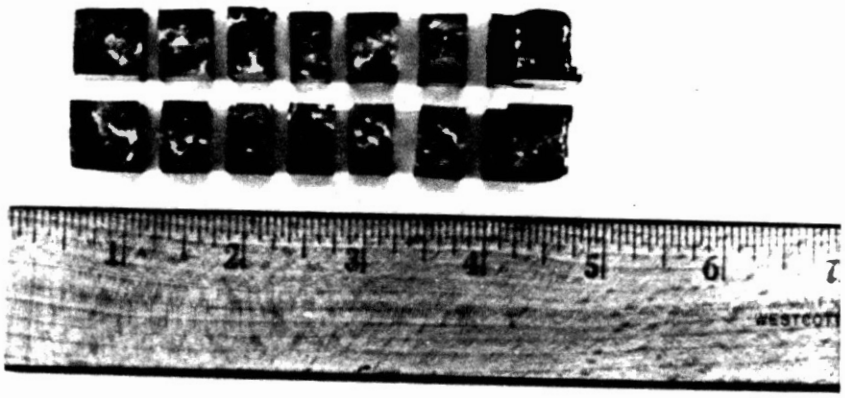

Figure 13. Cast specimen fully sectioned for heat treatment and evaluation.

Heat Treatment Cycles Performed

To make an evaluation of the effects of heat treatment on the ferrite present in the as-cast microstructure, several variables had to be considered. These include the temperatures, the number of different temperatures, the times, the heat treating atmosphere, and, the quenching media. These variables were determined and the 24 specimens were heat treated.

The first variable to be considered is the temperatures at which the heat treatments should be done. Since standard heat treating practice for CF-3M castings states 1900°F(1040°C) as the minimum temperature it was chosen as a starting point (ASTM A743).

The next variable is the number of different temperatures. Of course, this is related to the number of available sections. Since each specimen was cut into six sections and five or six points should make fairly nice data sets for each temperature, four heat treating temperatures with five different times at each one are in order. The temperatures were then chosen as follows: 1900°F(1040°C), 1950°F(1066°C), 2000°F(1093°C), and 2050°F(1121°C). One additional point which must be made here is the amount of control of the selected temperatures in the furnace during the heat treatment cycles. Immediately following loading or unloading of a

section, the furnace took about 30 to 45 seconds to stabilize to steady operation.

The atmosphere used in the heat treating procedure was normal air. Air was chosen both because it was acceptable according to standard heat treating practices and because of difficulties associated with inert environments (ASTM A743).

Finally, the last and most difficult variable to be considered is the heat treatment times. Standard heat treatments do not give time requirements other than some statement about enough time for complete heating or heating through the thickness. Therefore, a need for a procedure to determine suitable times to cause change in the ferrite structure was needed. To meet this need the following procedure was developed. First, two sections were heat treated at the lowest temperature, one for two minutes, the other for ten minutes. Ferrite estimates were then made from these two times. Since the dissipation of the ferrite is expected to follow a psuedo-rate equation, which would mean the fraction of the ferrite remaining should fall along a straight line when plotted against the log of the time, the resulting ferrite could be estimated from the first two points. This done suitable times could be estimated and performed for the first temperature. Then, using the results from the first temperature, suitable times for subsequent temperatures could be

determined. A summary of the times and temperatures can be found in the next chapter.

Metallographic Preparation of Specimens

The metallographic preparation of the specimens consisted of several stages. First, work was done to determine a suitable etchant. Then the heat treated sections were mounted, polished, and etched. Vilella's reagent was chosen as a suitable etchant, it consists of 1g Picric acid, 5ml HCl, and 100ml Methanol. Vilella's reagent produces very nice and repeatable results simply by immersing the specimen for 3-4 minutes then rinsing with water and methanol.

After heat treatment the specimens were mounted in two part epoxy cold-mounts. Next, the specimens were ground on successively finer grit paper down to 600 grit. Then, they were polished with 5 micron and 1 micron alumina polish successively on long nap polishing wheels; and finally, they were etched as described above in Vilella's reagent.

Microstructural Evaluation of Specimens

The morphology of the ferrite pools in the austenite matrix refers to the amount and the configuration of the ferrite pools. Since both of these are to be studied, both will need to be evaluated.

The volume percent of the ferrite can be estimated

with some degree of accuracy using a manual point count method which was mentioned earlier but is described in in the Appendix. Estimations made by this method were verified to some extent by comparison with the ferrite number which was estimated from the composition using the Schoeffer diagram.

While the amount of ferrite can be estimated with some degree of accuracy, the configuration of the ferrite is more difficult to characterize quantatively. Therefore, observations of the changes were made and recorded and photographs were taken of significant features.

CHAPTER V

RESULTS OF EXPERIMENTAL WORK

Introduction

The experimental work which was outlined in the previous chapter produced two major categories of results which are reported in this chapter. The first is a set of observations concerning the defects observed in the castings. The second consists of two parts, a complete record of the ferrite numbers observed in the samples after undergoing various heat treating cycles and the set of observations and photographs taken to record the changes produced in the morphology of the cast structure during heat treatment.

Defects Observed in the Castings

Several of the defects observed in the castings were expected, however a few were unexpected. The most obvious defect found in these castings was not actually a defect in that it was expected, planned for and did not have a detrimental effect on the project. This defect was the poor surface finish. It is reported here only because it was far rougher than is normally expected in an investment casting. Another defect which

was very obvious upon sectioning was the large shrinkage cavity present at the intersection of the plate and the riser. However, like the surface finish this defect was also planned for and caused no ill effects on the project.

While the surface finish and the large shrinkage cavity were expected, two other types of defects were observed which were unexpected but did not cause any problems. These were a number of minor inclusions and small pits. There was an occasional very small inclusion present in the castings. These did not cause any problems with the project because there were very few and the could pretty much be ignored. Likewise, the small pits caused very little concern because while they were seldom located closer than 800 - 1000 microns from each other. The inclusions were probably caused by loose pieces of mold material that became entrained in the molten metal flow. While the small pits were probably due to interdendritic porosity. This is reasoned due to their location between the dendrites.

Delta Ferrite Observations

The delta ferrite observed in the cast specimens of CF-3M looked very much like the structures reported by David, refer to Figure 7. The delta ferrite appeared as dark pools in a light colored matrix of austenite when the specimens were etched with Vilella's reagent. In

this section the ferrite estimations made of the various specimens will be reported and the changes observed in the morphology of the ferrite will be presented.

As described in the previous chapter the volume percent of the ferrite present was estimated for the various specimens using the manual point count method. The volume percent ferrite was also estimated by taking an average of an estimate made near each of the other sets of specimens and was found to be 12.85% with a 95% confidence interval of 0.449%, which agrees fairly well with the estimate of 12.29% determined using the Schoeffer diagram. As explained in the Appendix , the manual point count relies on a statistical estimation of the actual volume, therefore a confidence interval must also be reported with the estimate. In this case a 95 percent confidence interval was reported. Table 3 is a summary of the ferrite estimates and the confidence intervals which are related to each estimate.

TABLE 3

VOLUME PERCENT FERRITE ESTIMATES

1900°F(1040°C)					
time	2 min	10 min	30 min	100 min	300 min
% ferrite	12.60	10.17	9.35	7.07	5.24
C. I.	0.922	0.700	1.060	0.790	1.150

1950°F(1066°C)

time	3 min	10 min	30 min	100 min	200 min
% ferrite	9.52	9.18	6.80	5.48	4.93
C. I.	1.010	1.010	0.970	0.743	0.620

2000°F(1093°C)

time	3 min	10 min	30 min	60 min	150 min
% ferrite	9.52	7.99	5.71	4.90	4.08
C. I.	0.891	0.692	0.653	0.680	0.585

2050°F(1121°C)

time	3 min	6 min	15 min	30 min	60 min
% ferrite	9.86	8.20	4.49	3.98	3.64
C. I.	1.240	0.914	0.490	0.446	0.511

From the estimates of both the as-cast and the heat treated percent ferrite counts, plots of f/f_o vs. log time could be made for each heat treating temperature. Where f/f_o is the fraction of the ferrite remaining and the time refers to the actual amount of time in the heat treating furnace. The plots for the various temperatures can be seen in Figures 14 through 17. The vertical bars indicate the corrected 95% percent confidence interval. The corrected 95% confidence interval is calculated to guarantee that both the confidence interval for the numerator and the

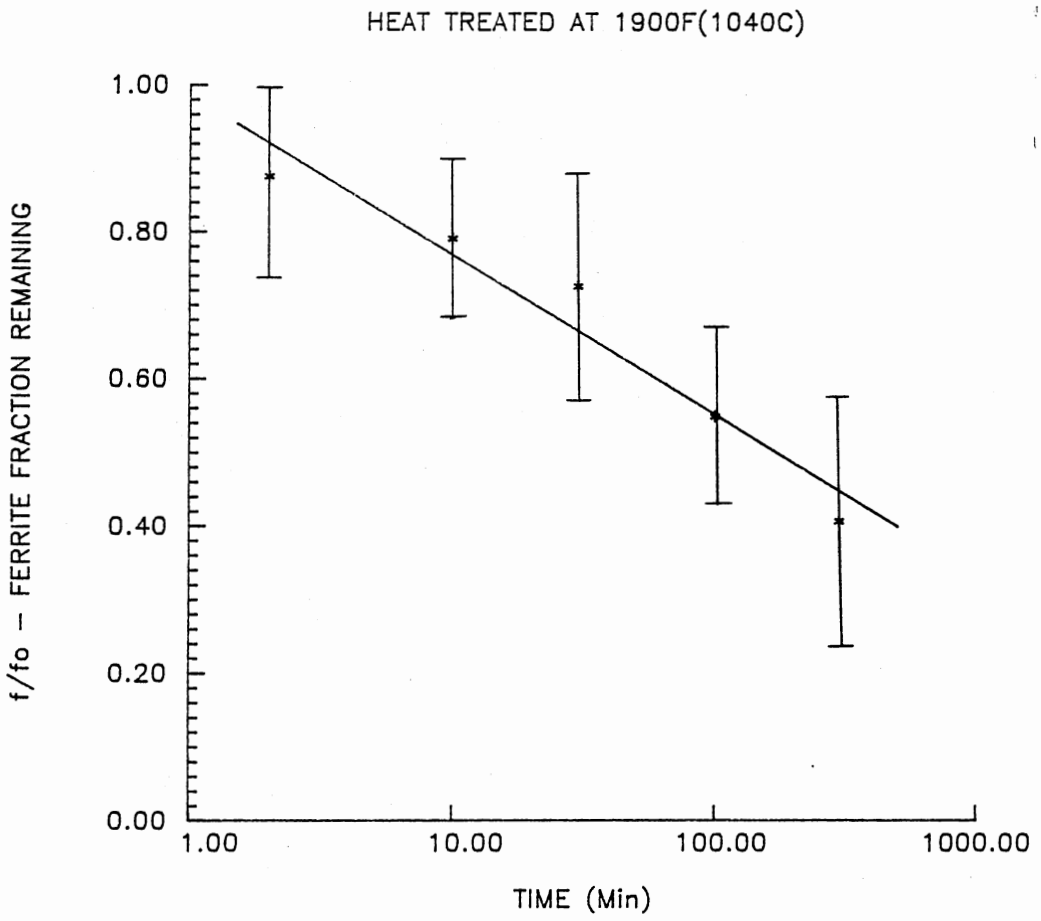

Figure 14. Ferrite dissolution data for specimens heat treated at 1900°F(1040°C).

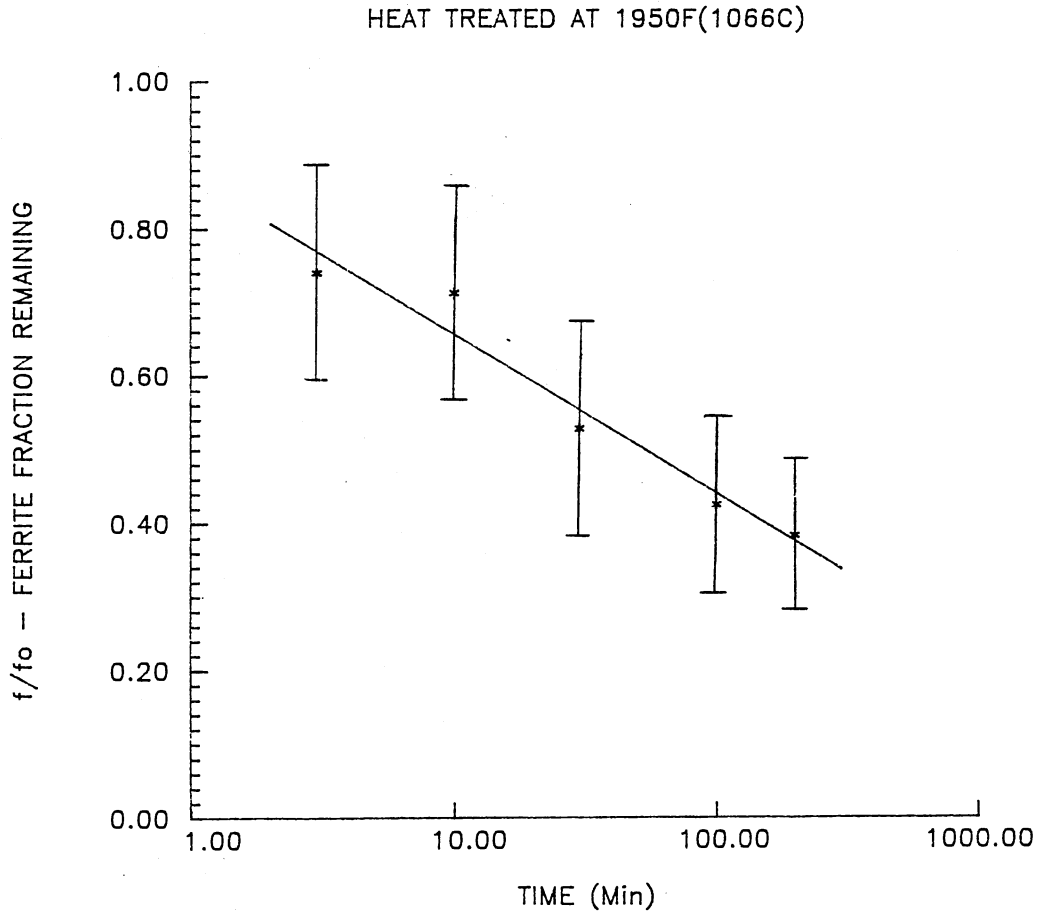

Figure 15. Ferrite dissolution data for specimens heat treated at 1950°F(1066°C).

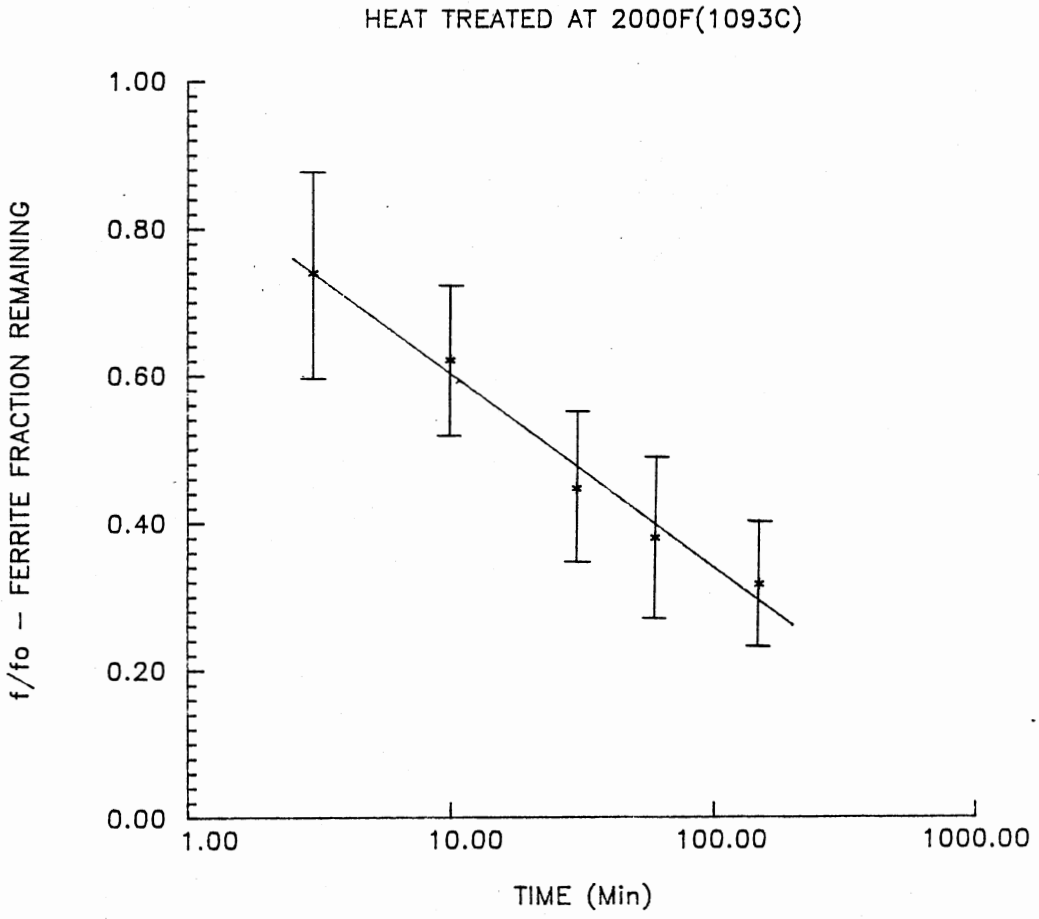

Figure 16. Ferrite dissolution data for specimens heat treated at 2000°F(1093°C).

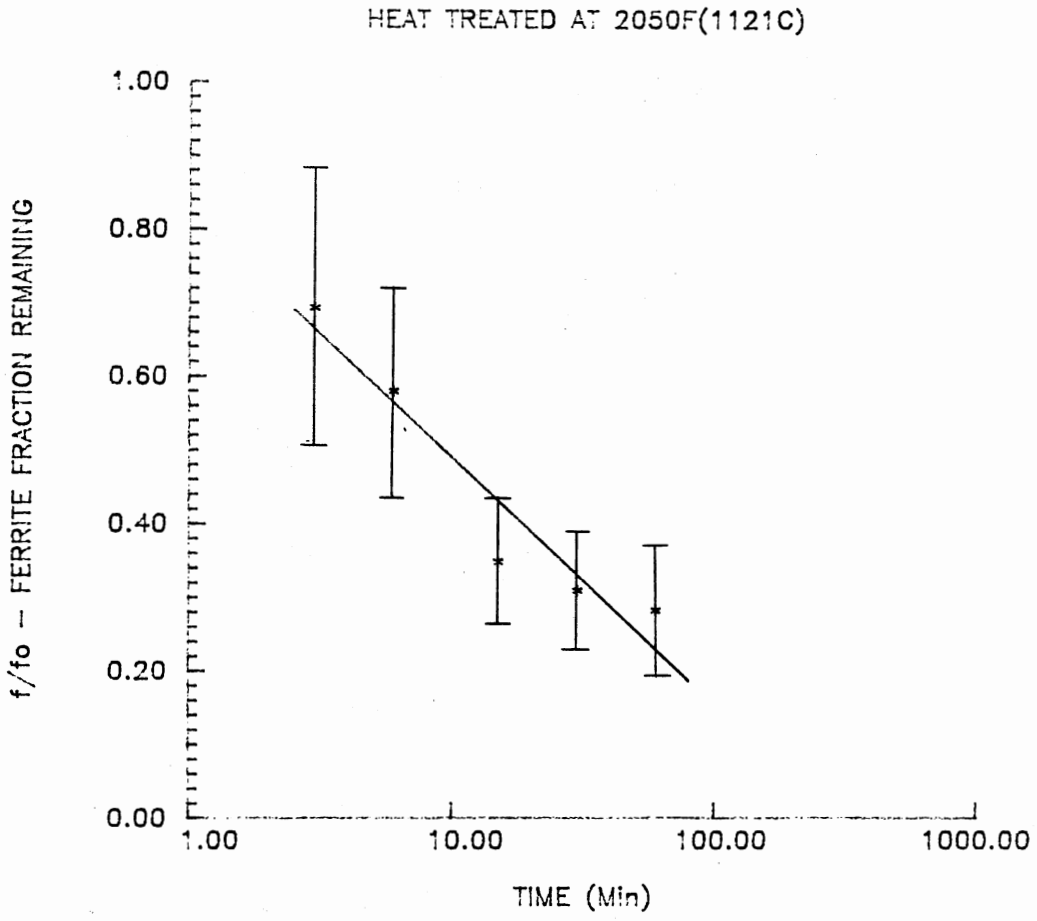

Figure 17. Ferrite dissolution data for specimens heat treated at 2050°F(1121°C).

denominator are covered. Figure 18 is a composite of the four previous plots again showing the fraction of the ferrite remaining as a function of time. In this case the confidence intervals were omitted for clarity. A straight line was fitted through each of the sets of data. The line in each case is at the best location which was determined using linear regression. A straight line was chosen because a line seems to fit fairly well in all of the cases, it stays within the confidence interval, and because, in the past, the dissolution of ferrite has been shown to follow a pseudo-rate equation, that has a straight line form.

The changes in the morphology of the delta ferrite during the various heat treatment procedures was also observed. A series of photographs was taken at each of the times used for the 2050°F(1121°C) group. This series is representative of the changes seen at the other temperatures concerning the manner by which the ferrite changes. Figures 19 through 24 show the progress of the ferrite dissolution. The photograph in part a of each of these figures is of the vermicular structure which is located only along the surface of the specimens, while the photograph in part b of each of these figures is of the lacy structure which is located in the center regions of the specimens. Very close similarities can be seen to exist between these structures and those contained in Chapter III which were

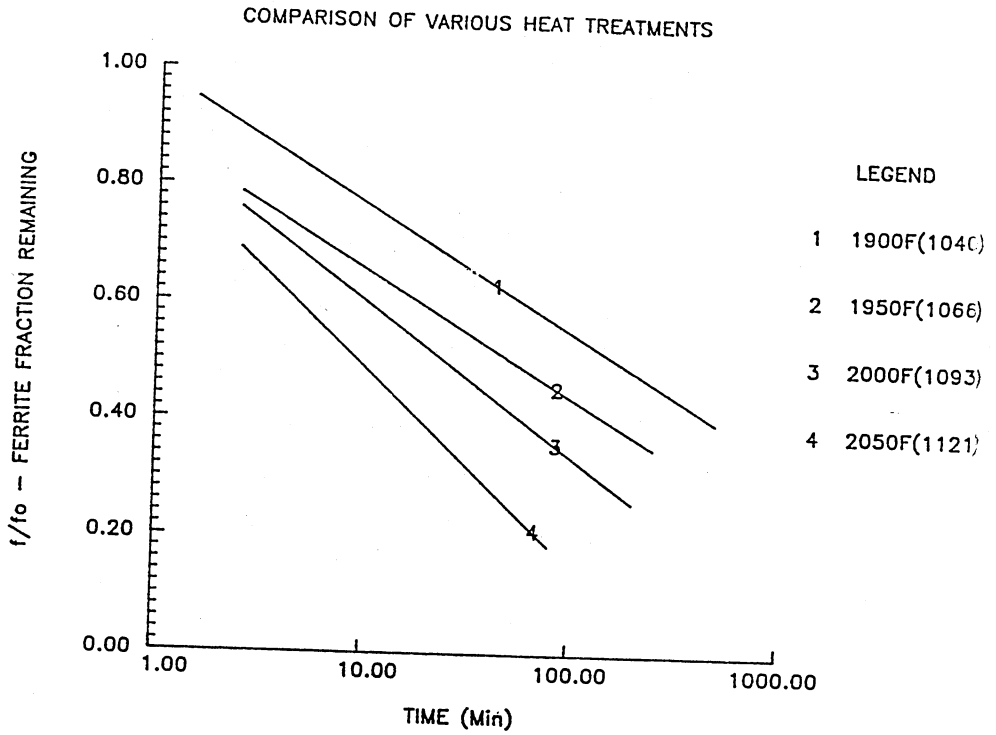

Figure 18. Comparison of the ferrite dissolution data for various heat treatments.

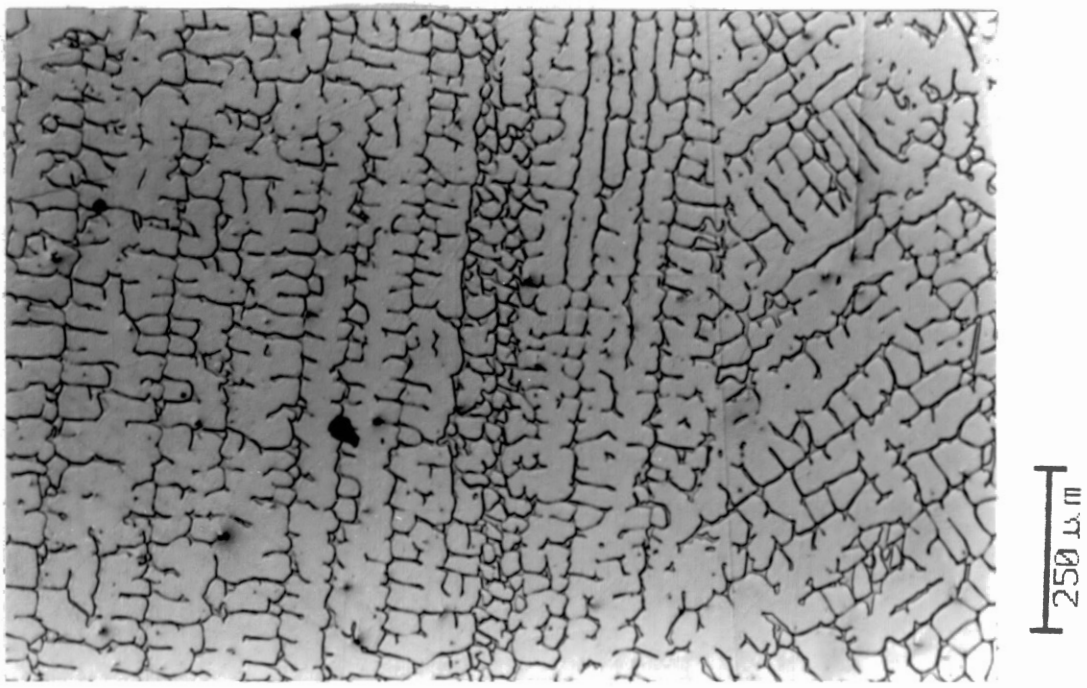

Figure 19a. Vermicular structure in the as-cast condition.

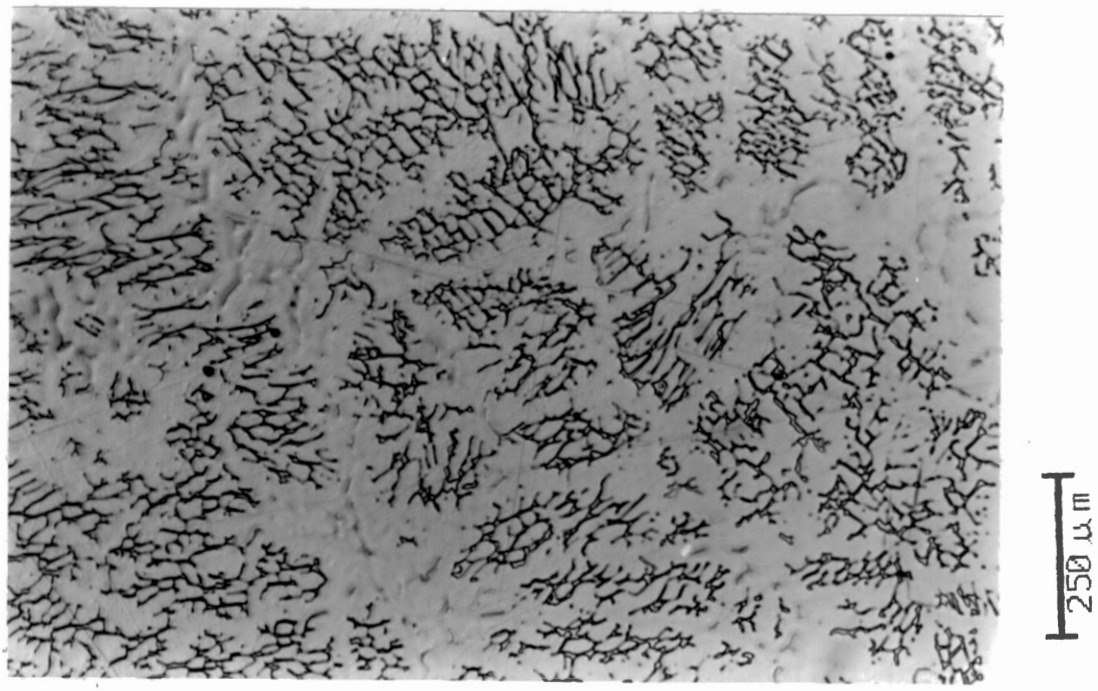

Figure 19. Lacy structure in the as-cast condition.

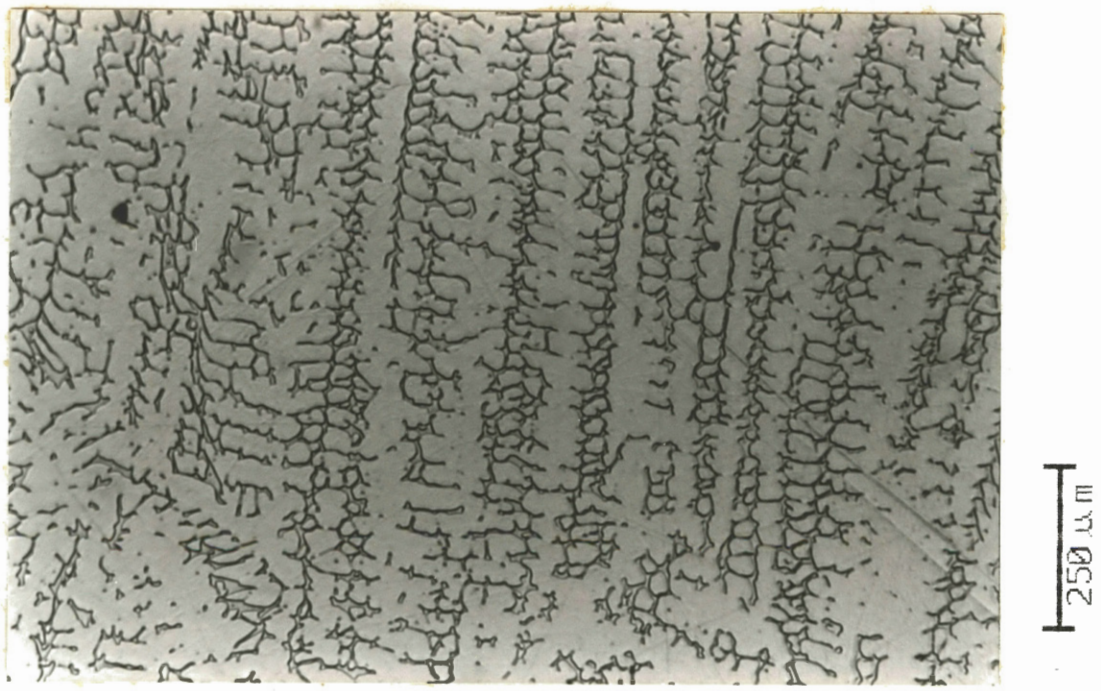

Figure 20a. Vermicular structure heat treated 3 minutes at 2050°F(1121°C).

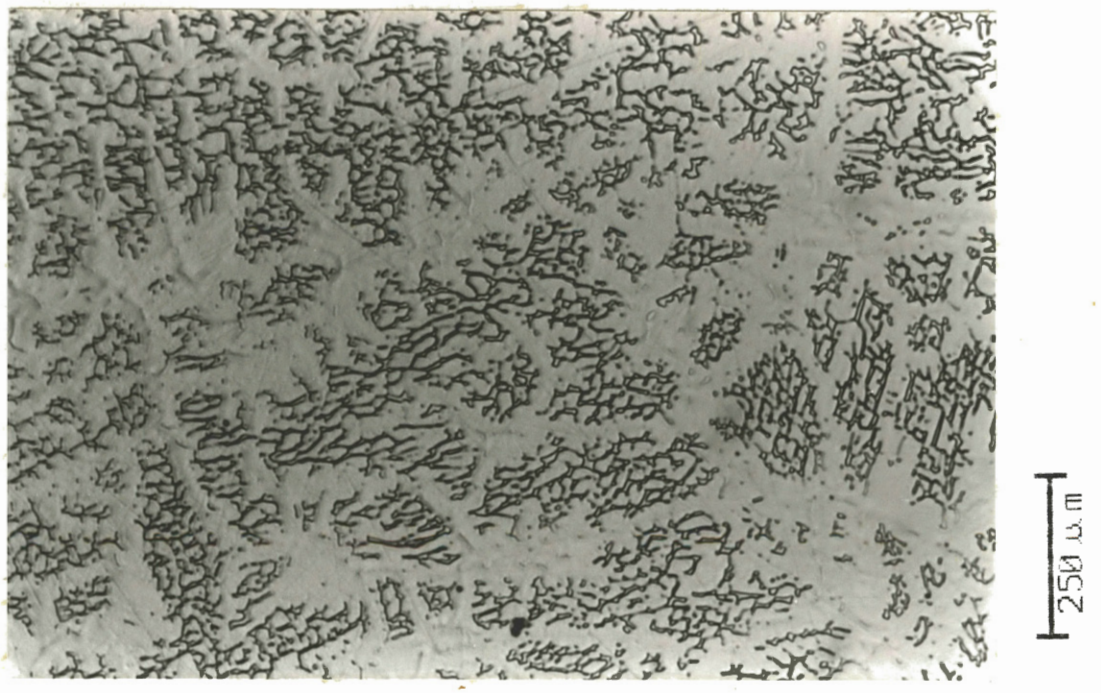

Figure 20b. Lacy structure heat treated 3 minutes at 2050°F(1121°C).

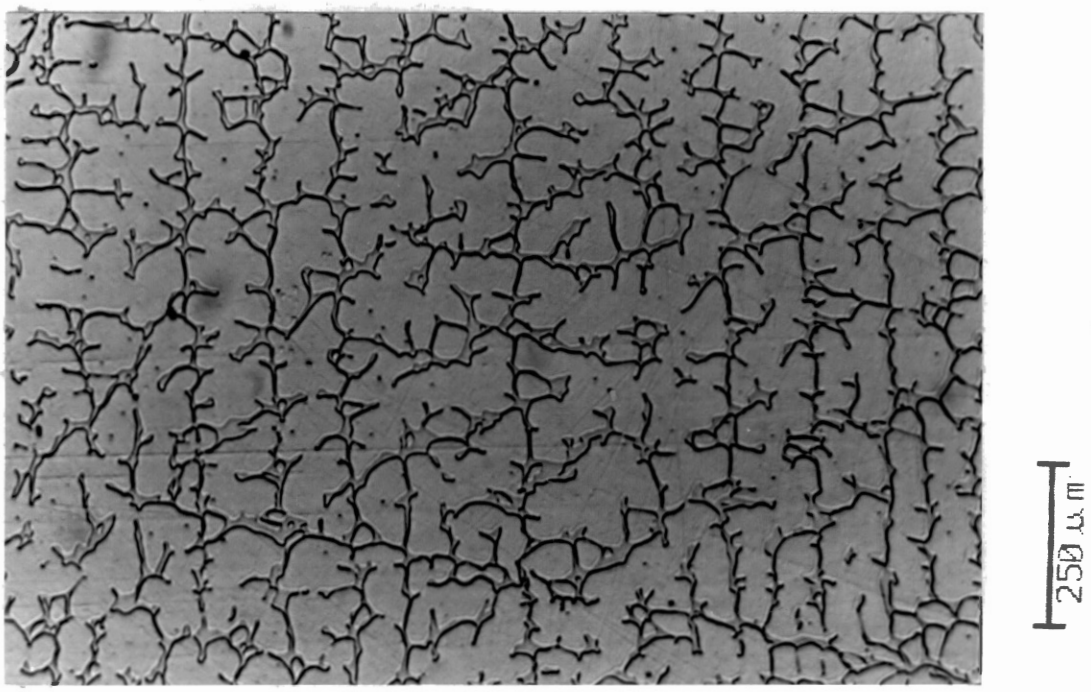

Figure 21a. Vermicular structure heat treated 6 minutes at 2050°F(1121°C).

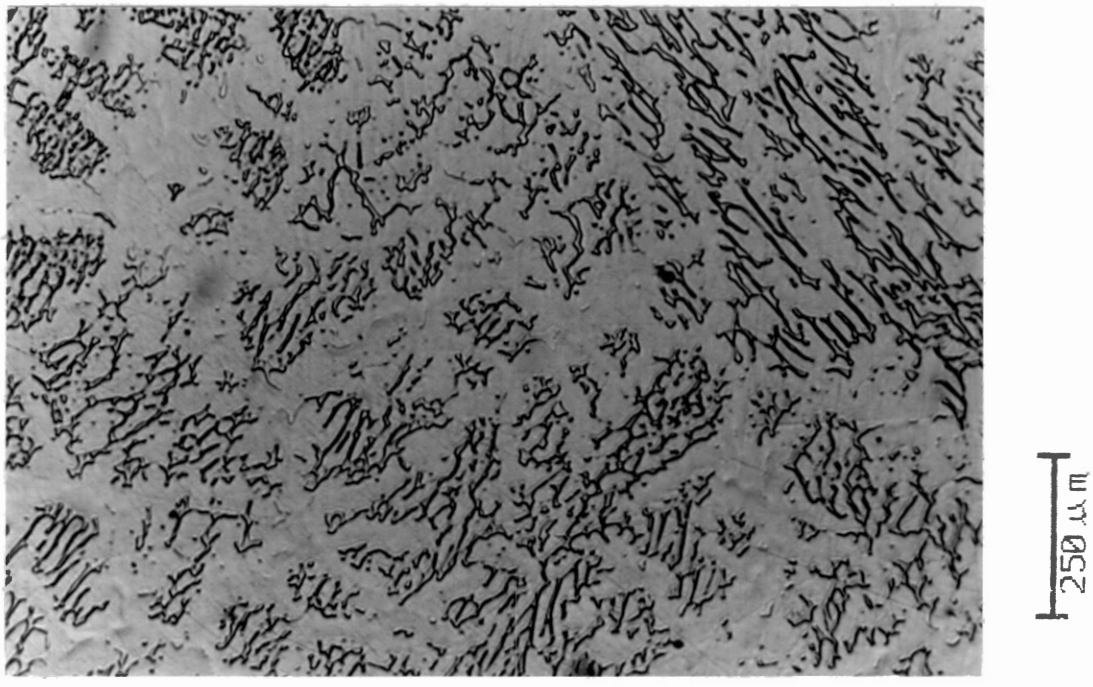

Figure 21b. Lacy structure heat treated 6 minutes at 2050°F(1121°C).

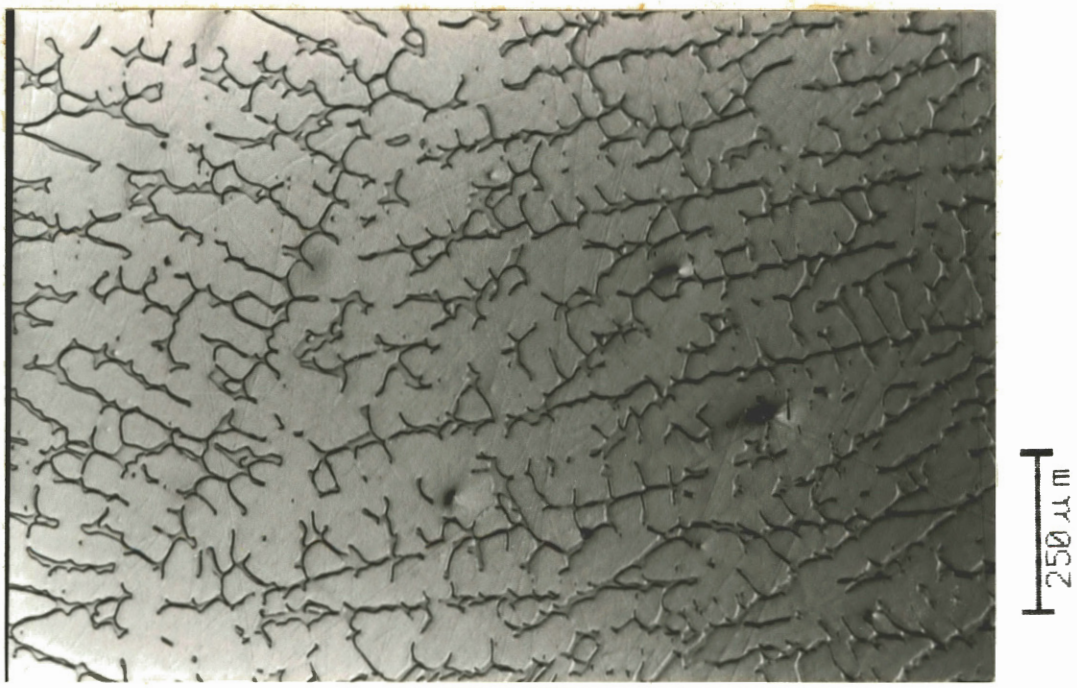

Figure 22a. Vermicular structure heat treated 15 minutes at 2050°F(1121°C).

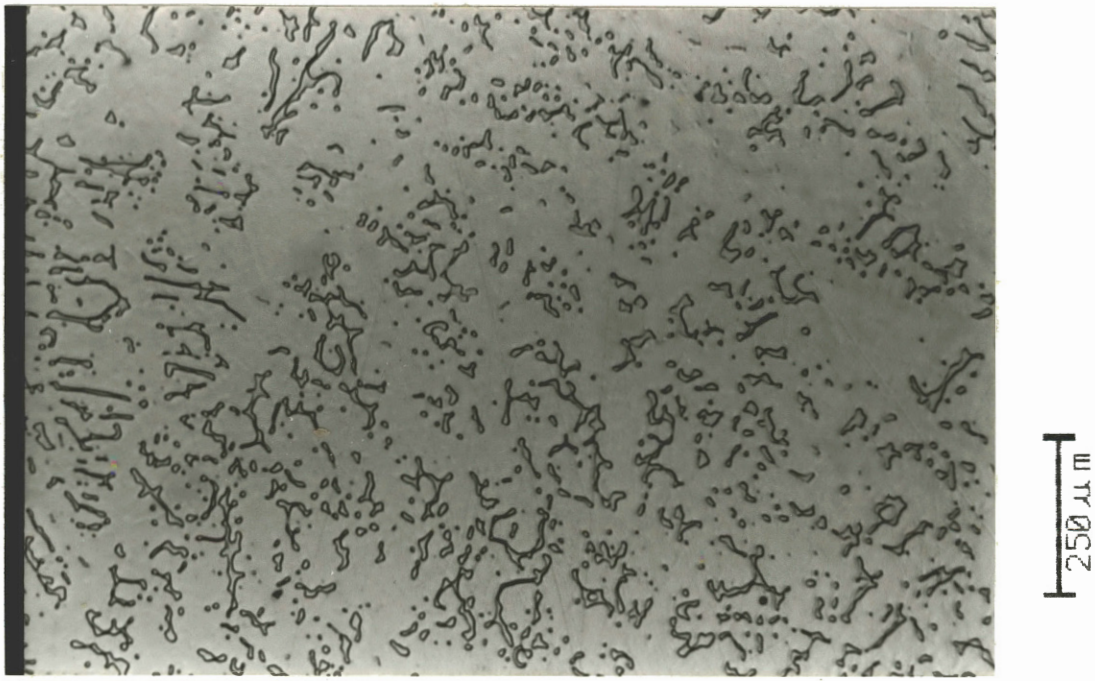

Figure 22b. Lacy structure heat treated 15 minutes at 2050°F(1121°C).

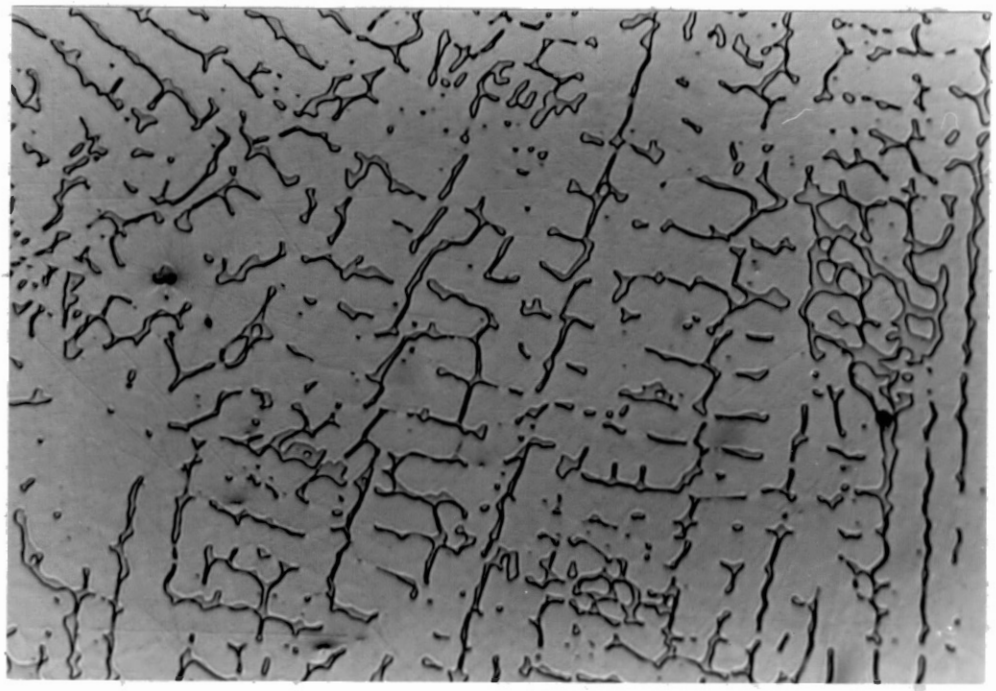

Figure 23a. Vermicular structure heat treated 30 minutes at 2050°F(1121°C).

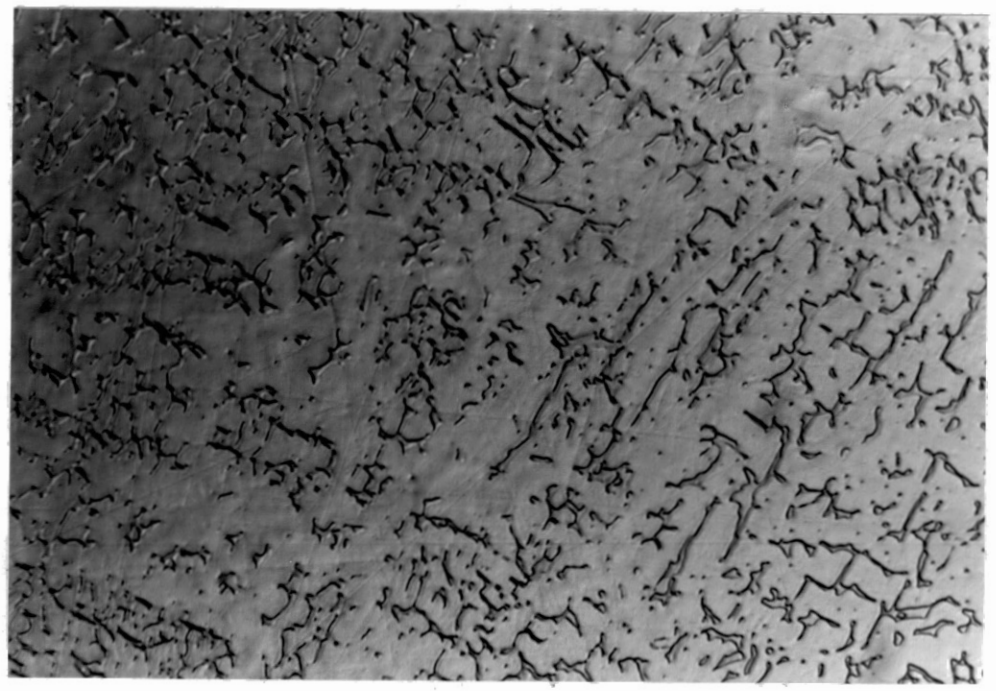

Figure 23b. Lacy structure heat treated 30 minutes at 2050°F(1121°C).

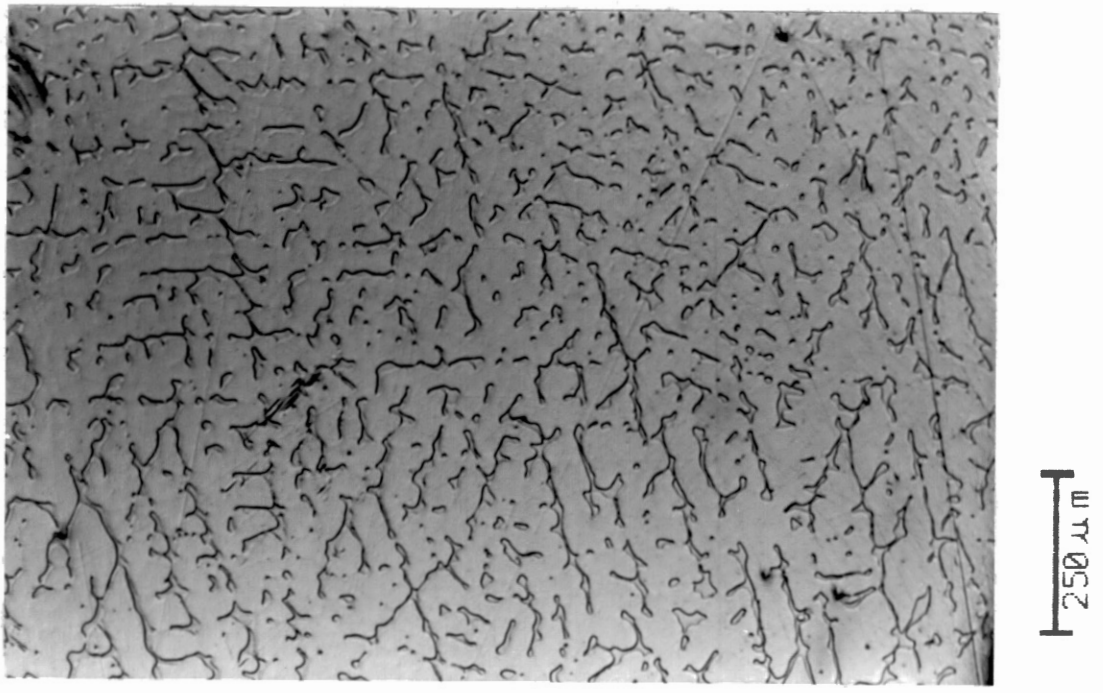

Figure 24a. Vermicular structure heat treated 60 minutes at 2050°F(1121°C).

Figure 24b. Lacy structure heat treated 60 minutes at 2050°F(1121°C).

reported by David. In general it appears that the pools of ferrite simply dissolved as the heat treatments took place. It seems that some amount of spherodization did take place especially in the final stages. However, the globular shaped pools which do remain are hardly larger in diameter than the original structures were thick. It appears that the lacy structure progressed in the dissolution process at a slightly higher rate than did the vermicular structure; however, when estimates were made in the regions separately, no difference could be resolved outside of the 95% confidence interval. This dissolution process caused the ferrite pools to change shape as they were dissolving, apparently with the thinner sections dissolving first leaving the heavier sections. Figure 25 is a schematic representation of this process taking place in the vermicular structure. The arrows indicate the progression of time. Again, notice how the smaller parts dissolve first leaving only the heavier parts. Since the ferrite pools appear to be the remnants of the original delta ferrite dendrites and appear to be on the cores of the original dendrites, the small parts which dissolve first are the cores of the secondary dendrite arms.

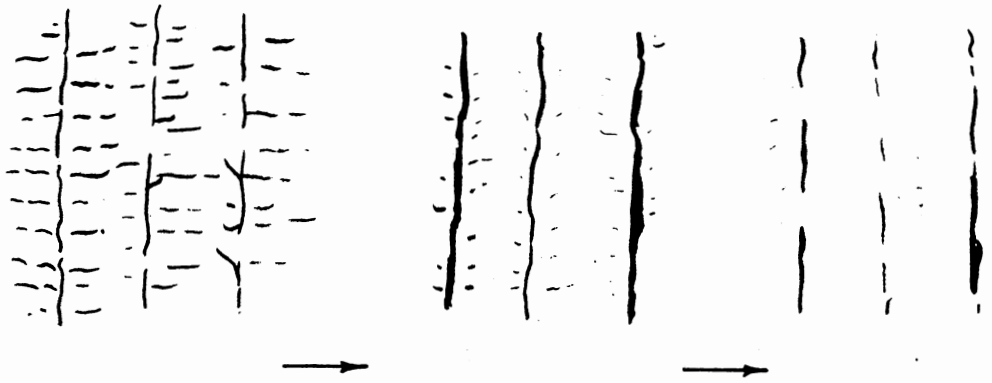

Figure 25. Schematic of ferrite dissolution. Arrows indicate increasing time at temperature.

CHAPTER VI

DISCUSSION AND RECOMMENDATIONS

Introduction

The results of the experimental work were reported in the last chapter. This chapter is a discussion of those results. A discussion of the ferrite depletion and of the change in morphology is presented and recommendations for further work are made.

Discussion of Ferrite Depletion

As is obvious from the data and the photographs presented in the last chapter, the delta ferrite depletes with time during a heat treatment process. It has been put forth that this process is diffusion controlled. This certainly makes sense based on the information concerning the partitioning of the elemental components in the as-cast structure. This section presents the analysis of the data to determine the activation energy of the diffusion process. Then these results and their impact will be discussed.

As was discussed in Chapter III Leone and Lippold have both shown that the cores of the original ferrite dendrites which are left as ferrite are enriched in

ferritizers while the original interdendritic regions are enriched in austenizers (Leone 1982, Lippold 1979). This of course would mean that a differential is set up that will allow diffusion to take place and cause changes in the concentrations in the various regions. This is one driving force; however, another one exists. This other driving force for ferrite dissolution is that the metastable delta ferrite has a higher energy level than does the dissolution products.

It is expected that the amount of segregation and the energy level of the metastable delta ferrite is dependent on the history of the structure. For instance, a structure that was cooled at equilibrium conditions will have a much lower final energy level than one that was quenched. Further solidification rate and temperature gradient is also expected to play a role on the amount of segregation that is present in the as-cast structure. From these two points of conjecture one can reason that the reaction to heat treatment of structures which were cast in various ways will differ. This variation is not addressed in this study.

There are many things which may affect the rate of dissolution of the ferrite into austenite. For example, the carbides which percipitate in the ferrite will be dissolved during the time the ferrite is being transformed to austenite. This means that the carbon is forced to relocate itself as the structure changes pahse

also the free chromium resulting from the decomposition of the carbides serves to further stabalize the ferrite.

The overall activation energy of the process can be calculated from the data reported in the last chapter. This calculation is based on equation 2 which is similar to the Arrehnius equation but is different in that the diffusion coefficients are replaced by a rate coefficient that is not a pure diffusion coefficient. This difference is further compounded by the factors just mentioned. This equation was given in Chapter III as:

$$K_D = K_{D_o} \exp(-Q/RT) \qquad (2)$$

The K_D for each temperature is the modulus of the slope of the line for each set of data that was presented in the last chapter. Table 4 gives a summary of this information. To determine Q, the best fit line is found through the data points as they would be plotted as $\ln(K_D)$ vs $1/T$ where T is absolute temperature. The slope of this line is equal to the Q/R, where R is the ideal gas constant. In equation 2, Q refers to the activation energy which is the amount of energy which must be added to the system to cause it to shift from a metastable plateau to a stable valley. This value is easy to determine and was found to be 80 KJ/mol. This activation energy is quite a bit lower that the 132 KJ/mol activation energy that Raghunathan found for the

dissolution of ferrite in the weld metal of type 316 stainless steel (Raghunathan 1979). This lower value for the overall activation energy in this process is not surprising considering that the structure found in weld metal would have solidified under much more transient conditions and that it would have more carbides present. The other variables mentioned earlier would also act to decrease the expected activation energy for this process.

TABLE 4

K_D VS TEMPERATURE DATA

Temp (K)	10^4 / T	K_D	ln K_D
1313	7.616	0.2226	-1.502
1339	7.468	0.2158	-1.533
1366	7.320	0.2619	-1.340
1394	7.174	0.3349	-1.094

While the activation energy and the rate equations do a fairly good job of predicting the rate of decay of the ferrite into austenite during heat treatment, the issue of how much ferrite is needed still is unanswered. This is a difficult question and is beyond the scope of this study. However, it should be clear that if reliable tests were performed which could predict the optimum ferrite level for a certain casting and casting

condition, then a set of tests such as these could also be done and the results used to predict the necessary heat treating conditions to yield the desired amount of ferrite.

Discussion of Ferrite Morphologies

For some time it was commonly thought that the differences in morphology observed were actually only due to the relative orientation of dendrites. However, David has presented a full discussion of various morphologies. The results of his work are presented in the third chapter of this study and are shown in Figure 7.

Some differences appear in the two microstructures during heat treatment. It appears, when observing the microstructures visually, that the lacy morphology dissolves more quickly than the vermicular morphology. However, no difference could be measured between the two regions using the manual point count method. Therefore, it can be reasoned that the difference in appearance of these two regions is due to the lacy morphology dissolving in a slightly different fashion, resulting in a greater number of smaller residual pieces which would give the appearance of less ferrite.

One point that should be made about the dissolution of the two morphologies originally present in the microstructure, is that they both tend to progress

toward a morphology that is more spherodized than the original. This may yield some advantage toward improving the crack initiation properties of the material. This advantage stems from the fact that the rounded ends of a sphere shaped pool will be less likely to initiate a crack than many of the sharper corners on the lacy and vermicular structures.

Recommendations for Further Work

The concerns with ferrite dissolution and the issues of the ferrite content in austenitic stainless steel weldments has received considerable attention. While a weld is in effect a small casting, the solidification conditions are very different from those of standard casting processes. Areas more specific to castings still need specific work. One such area would be a study of the effects of solidification rate and temperature gradient on the ferrite content and morphology, and a second area would be a study of the effects that various delta ferrite amounts and morphologies have on mechanical properties of the as-cast and heat treated material.

CHAPTER VII

SUMMARY AND CONCLUSION

A casting was designed which could be sectioned to provide a set of test specimens which could be used in microstructural evaluations. Wax patterns were made of the casting design, they were assembled into a tree and an investment shell mold was built-up around them. The wax pattern was removed and the mold was prepared to have the molten metal poured into it. CF-3M stainless steel was poured into the mold at 2714°F(1490°C). The casting was removed from the mold, cleaned, and sectioned for microstructural evaluation. Upon initial examination it was determined that only two of the morphologies which were previously reported in the weld microstructure by David were present in the cast microstructure. The test specimens were divided into four groups and the specimens from each group were heat treated for various times at 1900°F(1040°C), 1950°F(1066°C), 2000°F(1093°C) and 2050°F(1121°C). The individual specimens were examined metallurgically and the volume percent ferrite was calculated for each one. It was found that the fraction of ferrite remaining obeys a pseudo-rate equation which relates it to the log

of the time of the heat treatment. Further, from the four temperatures it was possible to calculate the overall activation energy for the dissolution process of the ferrite into the austenite matrix and it was found to be 80 KJ/mol. This value is lower than other similar figures in the literature but it was reasoned that this was due to the different histories of the structures. The morphology of the ferrite microstructure was also observed and it was found that during the dissolution process the various morphologies of the ferrite all tend to lose their elongated shapes and move toward spherodization. This softening of the ferrite phase may in itself produce some beneficial mechanical properties. Since it eliminates the sharp corners and ends, the likelihood of the ferrite phase initiating or aiding in the propagation of a crack is greatly reduced. Further, it was observed that this process progresses in a slightly different manner in the different morphologies with the lacy morphology breaking into a finer dispersion and the vermicular structure spherodizing as a larger globules. This difference between the morphologies may possibly cause differences in the mechanical properties between the two morphologies after heat treatment. Since the pools of delta ferrite act as second phase strengtheners, it is very likely that while there is no significant difference in the amounts of ferrite in the two distinct morphologies the finer more

dispersed pattern observed in the lacy morphology will probably better enhance the mechanical properties.

BIBLIOGRAPHY

ASM. Metals Handbook - Atlas of Microstructures. 8th ed. Vol. 7. Metals Park, Ohio: American Society for Metals, 1972.

ASM. Metals Handbook - Properties and Selection of Stainless Steels, Tool Materials and Special Purpose Metals. 9th ed. Vol. 3. Metals Park, Ohio: American Society for Metals, 1980.

ASM. Metals Handbook - Metallography and Microstructure. 9th ed. Vol 9. Metals Park, Ohio: American Society for Metals. 1985.

ASTM, A743. "Standard specifications for castings, iron-chromium, iron-chromium-nickel, corrosion resistant, for general application." 1988 Annual Book of ASTM Standards. Vol. 01.02. American Society for Testing and Materials, 1988.

ASTM, A800. "Standard practice for steel casting, austenitic alloys, estimating content thereof." 1988 Annual Book of ASTM Standards. Vol. 01.02. American Society for Testing and Materials, 1988.

ASTM, E562-83. "Standard practice for determining volume fraction by systematic manual point count." 1988 Annual Book of ASTM Standards. Vol. 01.02. American Society for Testing and Materials, 1988.

ASTM-STP 369. Advances in the Technology of Stainless Steel and related alloys. Philadelphia: American Society for Testing and Materials, 1965.

ASTM-STP 679. Properties of Austenitic Stainless Steels and Their Weld Metals. Philadelphia: American Society for Testing and Materials, 1979.

Bralower, P. M. "Casting clean steel." Modern Casting Feb. 1988, pp. 37 - 39.

Broad, E. M. "Investment casting process and its variables." Creative Manufacturing Seminars Technical Papers. #535. American Society of Tool and Manufacturing Engineers, 1967.

Budinski, K. Engineering Materials - Properties and Selection. 2ed Reston, Va.: Reston Publishing Co., a Prentice-Hall Co., 1983.

Campbell, H.C. "The ferrite problem - is it tempest in a teapot." Welding Journal, vol. 54 (1975): 867 - 871.

Cole, G.S. "Homogeneities and their control via solidification." Metallurgical Transactions, vol. 2, Feb. 1971. pp. 357 - 370.

Cottrell, A. An Introduction to Metallurgy. 2nd ed. London: Edward Arnold Publishers Ltd., 1975.

David, S. A. "Ferrite Morphology and Variations in ferrite content in austenitic stainless steel welds." Welding Journal, Vol. 60. April 1981. pp. 63s - 72s.

DeGroot, M. H. Probability and Statistics. Reading, Ma: Addison-Wesley Publishing Co., 1975.

DeLong, W. T. "Ferrite in austenitic stainless steel weld metal." Welding Journal, Vol. 53. 1974. pp. 273s- 286s.

Fisher, K. Fundamentals of Solidification. Switzerland: Trans Tech Publications SA, 1984.

Flemings, M. C. Solidification Processing. McGraw-Hill, 1974.

Fredriksson, H. "The solidification sequence in 18-8 stainless steel, investigated by directional solidification." Metallurgical Transactions, vol. 3. Nov. 1972. pp. 2989 - 2997.

Garrow, E. "Heat treatment of Investment cast stainless steels and high temperature alloys." Modern Casting. Dec. 1966. pp. 58 - 64.

Goodwin, G. M., Cole, N. C., Slaughter, G. M. "A study of ferrite morphology in austenitic stainless steel weldments." Welding Journal, vol. 51. 1972. pp. 425s - 429s.

Helmer, J. D. "Investment casting survey identifies industry needs." Modern Casting. July 1986. pp. 36 - 38.

Hilliard, J. E. and Cahn, J. W. "An evaluation of procedures in quantitative metallography for volume-fraction analysis." Transactions of the

Metallurgical Society of AIME., vol. 221. April 1961. pp 344 - 352.

Hull, F. C. "Effects of delta-ferrite on the hot cracking of stainless steel." Welding Journal, vol. 46. 1967. pp. 399s- 409s.

Irani, D. R. and Kondic, V. "Casting and mold design effect on shrinkage porosity of light alloys." Modern Casting. Dec. 1976. pp. 208 - 211.

Kotschi, R. M. and Loper, C. R. jr. "Effects of chills and cores on the design of junctions in castings." AFS Transactions. 1976. pp. 631 - 640.

Kalpakjian, S. Manufacturing Processes for Engineering Materials. Reading Ma.: Addison-Wesley Publishing Co., 1984.

Krohn, B. R. "The art and science of investment casting." Modern Casting. Dec. 1984. pp 22 - 26.

Leone, G. L. and Kerr, H. W. "The ferrite to austenite transformation in stainless steels." Welding Journal, vol. 61. Jan. 1982. pp 13s - 21s.

Lippold, J. C. and Savage, W. F. "Solidification of austenitic stainless steel weldments: part I - a proposed mechanism." Welding Journal, vol. 58. Dec. 1979. pp. 362s - 374s.

Ludema, K. C., Caddell, R. C. and Atkins, A. G. Manufacturing Engineering. Englewood Cliffs, NJ: Prentice-Hall, Inc., 1987.

Lula, R. A. New Developments in Stainless Steel Technology - Conference Proceedings. USA: American Society for Metals, 1985.

Marshall, P. Austenitic Stainless Steels - Microstructure and Mechanical Properties. New York: Elsevier Applied Science Publishers, LTD., 1984.

Minakawa, S., Samaraseker, I.V. and Weinberg, F. "Centerline porosity in plate castings." Metallurgical Transactions B, vol. 16B. Dec. 1985. pp. 823 - 829.

Moharil, D. B., Jin, I. and Purdy, G. R. "The effect of delta-ferrite formation on the post-solidification homogenization of alloy steels." Metallurgical Transactions, vol. 5. Jan. 1974. pp 59 - 63.

Murthy, K., Seshadri, M. and Ramachandran, A. "End chill thermal behavior and effects on casting soundness." Modern Casting. Nov. 1965. pp. 142 - 148.

Nereo, G. M., Polich, R. F. and Flemings, M. C. "Unidirectional solidification of steel castings." Modern Casting. Feb. 1965. pp. 57 - 69.

Pickering, F. B. ed. The Metallurgical Evolution of Stainless Steels. USA: American Society for Metals and The Metals Society, 1979.

Polich, R. F. and Flemings, M. C. "Mechanical properties of unidirectional steel castings." Modern Casting. Feb. 1965. pp. 84 - 89.

Raghunathan, V. S., Seetharaman, V., Venkdesan, S. and Rodriquez, P. "The influence of post weld heat treatments on the structure, composition and amount of ferrite in type 316 stainless steel welds." Metallurgical Transactions A, vol. 10A. Nov. 1979. pp. 1683 - 1689.

Ruddle, R. W. The Solidification of Castings. London: Institute of Metals, 1957.

Siegel, U., Spies, H. and Eckstein, H. "Effects of solidification conditions on the solidification sequence of austenitic chromium-nickel stainless steels." Steel Research, vol. 57. 1986, no. 1. pp. 25 - 32.

Suutala, N., Takalo, T. and Moisio, T. "Ferritc-Austenitic solidification mode in austenitic stainless steel welds." Metallurgical Transactions A, vol. 11A. May 1980. pp. 717 - 725.

Takalo, T., Suutala, N. and Moisio, T. "Influence of ferrite content on its morphology in some austenitic weld metals." Metallurgical Transactions A, vol. 7A. Oct. 1976. pp. 1591 - 1592.

Unterweiser, P. W., Boyer, H.E., and Kubbs, J. J. ed. Heat Treater's Guide - Standard Practices and Procedures for Steel. USA: American Society for Metals, 1982.

VanVlack, L. H. Elements of Material Science and Engineering. Reading, Ma.: Addison-Wesley Publishing Co. Inc., 1985.

VerSynder, F. L., Barlow, R. B., Sink, L. W., and

Piearcey, B. J. "Directional solidification in the precision casting of gas-turbine parts." Modern Casting. Dec. 1967. pp. 68 - 75.

Weiser, P. F. ed. Steel Casting's Handbook, 5th ed. Rocky River, OH: Steel Founder's Society of America, 1980.

APPENDIX

MANUAL POINT COUNT METHOD

The manual point count is specified in ASTM standard E562-83. According to Hilliard the systematic two dimensional point count is considered to be the preferable method to perform volume fraction analysis. Two other methods are the lineal method and the areal method. While these methods are far more complicated and time consuming they offer no advantage in accuracy over the manual point count method (Hilliard 1961).

The two dimensional systematic point count method is a reliable, unbiased method of estimating the volume fraction of a particular phase in a microstructure. In fact for a given number of observations the variance for the systematic point count is less than that for direct areal analysis. It should be understood that unbiased does not imply that the results will be error free but only that the expected result is equal to the true one. The statistical errors calculated with this method are only concerned with the method, in and actual analysis there will be a contribution to the variance from measurement errors. These may also lead to a biased estimate.

The principle behind the point count method is based on the stereological principle that a regularly spaced grid of points, when systematically placed over a two dimensional section through a microstructure, can provide, after a statistically representative number of placements, an unbiased statistical estimator of the volume fraction of an identifiable constituent phase.

Figure 26 shows a drawing of a two phase microstructure with a regular grid of sixteen points superimposed over it. The grid points which are circled touch the beta phase and are thus counted. Six points are on the beta phase and are counted, the points indicated with triangles are on a border and are thus counted as half. After summation, seven and a half total points touch the beta phase. The seven and a half is then divided by 16 and 46.9% is obtained for this observation. Next, enough observations must be made so as to be considered statistically large. Referring to ASTM E562 it is found that for this situation twenty to thirty observations should be made. Therefore, this counting procedure will need to be repeated from twenty to thirty times to obtain an estimate of the percent volume of the beta pahse present.

In this study the estimated amount of the ferrite was around 10% so a 49 point grid was chosen according to E562. The specification also recommends a minimum number of fields of 30. This should provide a

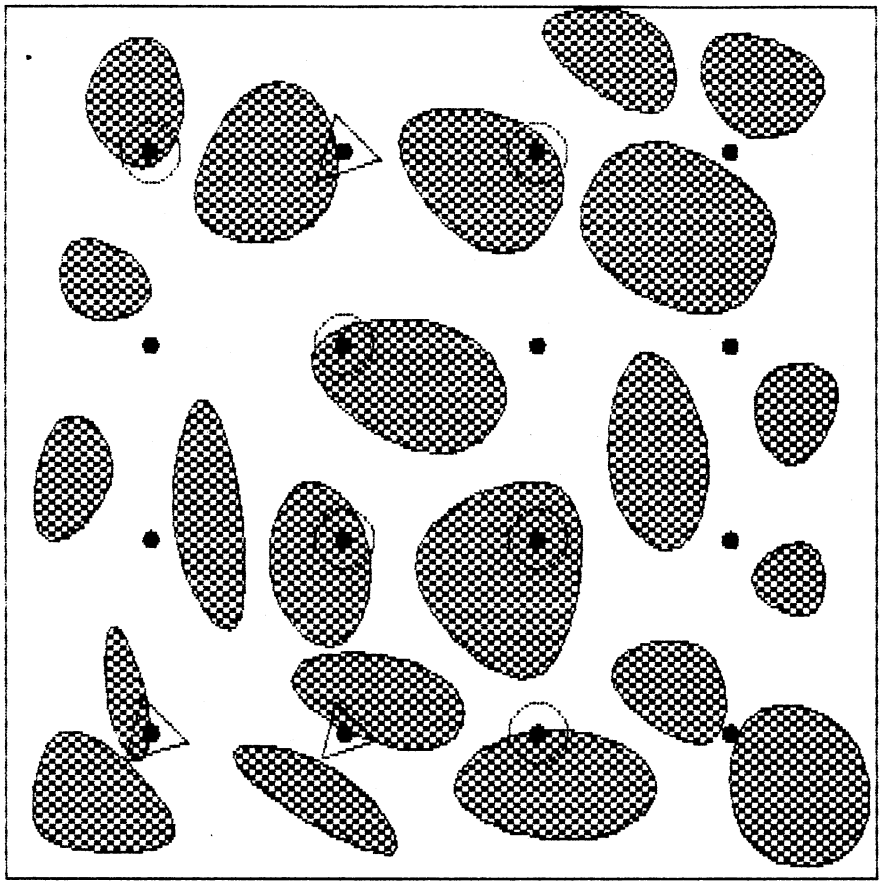

Figure 26. Two Phase Microstructure With Grid Superimposed.

reasonable expectation of obtaining a representative statistical sample which approaches large in the statistical sense. The data from a group of fields is analyzed statistically to determine the average, the standard deviation, and the 95% confidence interval as is recommended in the specification.

VITA 2

Paul D. Ratke

Candidate for the Degree of

Master of Science

Thesis: A STUDY OF THE EFFECTS OF HEAT TREATMENT ON DELTA-FERRITE IN CAST AUSTENITIC STAINLESS STEEL

Major Field: Mechanical Engineering

Biographical:

Personal Data: Born in Wichita Falls, Texas, September 7, 1965, the son of Henry and Ruby A. Ratke.

Education: Received Bachelor of Science Degree in Mechanical Engineering from Oklahoma State University in July 1987; completed requirements for Master of Science degree at Oklahoma State University in December 1988.

Professional Experience: Teaching Assistant, School of Mechanical and Aerospace Engineering, Oklahoma State University, June, 1987, to December 1987; Research Assistant, School of Mechanical and Aerospace Engineering, Oklahoma State University, January, 1988, to August, 1988.